Journal of Volcanology and Geothermal Research 438 (2023) 107806

Contents lists available at ScienceDirect

Journal of Volcanology and Geothermal Research

journal homepage: www.journals.elsevier.com/journal-of-volcanology-and-geothermal-research

The recent volcanism of Flores Island (Azores), Part II: Stratigraphy and eruptive history of the Comprida Volcanic System

Mariana Andrade [a,b,c,*], Ricardo Ramalho [d,a,b,e], Adriano Pimentel [f,g], Steffen Kutterolf [h], Armand Hernández [i]

[a] Universidade de Lisboa, Faculdade de Ciências, Instituto Dom Luiz (IDL), Campo Grande, Lisboa 1749-016, Portugal
[b] Universidade de Lisboa, Faculdade de Ciências, Departamento de Geologia, Campo Grande, Lisboa, Portugal
[c] Geosciences Barcelona (Geo3BCN-CSIC), Barcelona, Spain
[d] School of Earth and Environmental Sciences, Cardiff University, Park Place, Cardiff CF10 3AT, United Kingdom
[e] Lamont-Doherty Earth Observatory of Columbia University, New York, USA
[f] Instituto de Investigação em Vulcanologia e Avaliação de Riscos (IVAR), Universidade dos Açores, Ponta Delgada, Azores 9500-321, Portugal
[g] Centro de Informação e Vigilância Sismovulcânica dos Açores (CIVISA), Ponta Delgada, Azores 9500-321, Portugal
[h] GEOMAR Helmholtz Centre for Ocean Research, Kiel, Germany
[i] Universidade da Coruña, GRICA Group, Centro Interdisciplinar de Química e Bioloxía (CICA), Rúa as Carballeiras, A Coruña 15071, Spain

ARTICLE INFO

Keywords:
Ocean island volcano
Monogenetic volcanism
Hawaiian-Strombolian eruption
Phreatomagmatism
Glass geochemistry
Holocene volcanism

ABSTRACT

The stratigraphy and eruptive history of a volcanic system are key to forecast the timing and style of future eruptions. Flores is a small volcanic island in the Azores Archipelago with no record of eruptions since its settlement in the 15th century, although at least six eruptions are known to have occurred during the Holocene. Thus, Flores must be considered potentially active, and its volcanic hazard should not be disregarded. The most recent eruptions clustered at two centres of activity: the Funda Volcanic System (FVS) and the Comprida Volcanic System (CVS). Here, we reconstruct for the first time the eruptive history of CVS, the youngest volcanic system of Flores. Based on detailed tephrostratigraphic and geomorphological work, combined with radiocarbon dating and glass shard geochemistry, we show that – despite featuring five (maybe six) phreatomagmatic craters – CVS was formed in a single volcanic eruption at ~3180 cal yr BP. This eruption started with Hawaiian-style lava fountaining followed by Strombolian activity, dispersing tephra fallout across the central part of the island. Lava flows were also emitted during the initial phase, which drained to the west and cascaded over the older deposits of the massive slump of Fajãzinha–Fajã Grande, and possibly reached the coastline to form the Fajã Grande lava delta. The initial magmatic phase was followed by phreatomagmatic explosions that formed several maars and tuff rings. Hence, groundwater played an important role in the eruption by transforming a mild Hawaiian-Strombolian eruption into a highly explosive phreatomagmatic event, possibly due to oscillations in the eruption rate. The occurrence of a large landslide contemporary to the eruption, raises the possibility of a combined threat. A new and more robust volcanic hazard assessment for the island involving scientists and civil protection authorities is desirable.

1. Introduction

Knowledge of the stratigraphy and eruptive history of individual volcanoes or a volcanic region is one of the most important assets that scientists and civil protection authorities may hold in the attempt to forecast the timing and style of future eruptions and associated hazards (Andronico and Lodato, 2005; Martí et al., 2022; Barsotti et al., 2023). In active volcanic settings with recent eruptive activity, data from past eruptions can be obtained from historical documents and/or instrumental monitoring, but for older eruptions information is limited to the geological record. In the latter case, tephrostratigraphic and chronological studies are required to assess recurrence rates, styles, and magnitudes of past eruptions (McLean et al., 2020; Kisaka et al., 2021; Pedrazzi et al., 2022).

Unlike most other islands of the Azores Archipelago, Flores has no record of historical eruptions since the Portuguese settlement in the 15th

* Corresponding author at: Faculdade de Ciências da Universidade de Lisboa, Edifício C6, sala 6.2.79, Campo Grande, Lisboa 1749-016, Portugal.
E-mail address: mdandrade@fc.ul.pt (M. Andrade).

https://doi.org/10.1016/j.jvolgeores.2023.107806
Received 4 February 2023; Received in revised form 9 April 2023; Accepted 12 April 2023
Available online 17 April 2023

century, leading to the general perception that volcanism is dormant or extinct (Chester et al., 2017; Andrade et al., 2019). Accordingly, if compared with the central and eastern islands of the Azores, its volcanic hazard has often been underrated or overlooked. However, many volcanoes have periods of inactivity of thousands of years between eruptions (Scarpa and Gasparini, 1996), and therefore, all volcanoes that have erupted during the Holocene should be considered as potentially active. Because Holocene eruptions have been documented on Flores (Morisseau and Traineau, 1985; Azevedo and Portugal Ferreira, 1999; Andrade et al., 2021a, 2022) this island should be considered potentially active. The reconstruction of Flores' recent volcanic activity is, therefore, of utmost importance and should serve as the basis of a new, more robust volcanic hazard appraisal for the island.

Field evidence suggests that Flores experienced at least six eruptions during the Holocene, the latest occurring as recently as ~3000 years ago (Morisseau and Traineau, 1985; Andrade et al., 2021a, 2022). The most recent eruptions were centred at two clusters of activity, here denominated Funda Volcanic System (FVS) and Comprida Volcanic System (CVS), both of which were Strombolian and phreatomagmatic in style (Andrade et al., 2021a). Whilst the detailed eruptive history of FVS was recently reconstructed by Andrade et al. (2022), little is known about the volcanic activity that shaped the youngest CVS. CVS is nested within the volcano-sedimentary sequence of an old caldera, which hosts the upper groundwater body of the island (Azevedo, 1998), providing the favourable setting for phreatomagmatic interactions, with important hazard implications. In this study we reconstruct the eruptive history of the CVS and investigate how subsurface water can influence volcanic style, with the purpose of gaining insight into the likely hazards posed by possible future eruptions. We present for the first time a detailed tephrostratigraphy of the CVS, supported by radiocarbon dating and glass shard geochemistry, as well as estimates for the main physical parameters, providing data for a robust assessment of volcanic hazards.

2. Geological setting

The Azores Archipelago is situated in the North Atlantic Ocean, where the North American, Eurasian, and Nubian lithospheric plates meet (Fig. 1a). The Azorean islands are the result of volcanic processes related to the confluence of the three lithospheric plates and a mantle melting anomaly (Métrich et al., 2014; Genske et al., 2016). Flores is the westernmost island of the archipelago, and contrary to most of the other Azorean islands, it lies on the tectonically more stable North American plate, ~100 km west of the axis of the Mid-Atlantic Ridge (MAR) (Fig. 1a).

Flores volcanic edifice is formed by the products of overlapping shield and stratovolcanoes, with subaerial volcanism dating back to at least 2.16 Ma (Azevedo and Portugal Ferreira, 1999). The geological history of Flores was characterized by an initial phase that includes the products of both subaerial and submarine volcanic activity (2.16–0.75 Ma), followed by three long lasting phases of subaerial volcanic activity. The first (700–500 ka) was the most prominent and voluminous phase of volcanism of the island. It produced extensive and thick lava piles and pyroclastic deposits of basaltic to trachytic compositions. The second (400–200 ka) was dominated by effusive basaltic and hawaiitic volcanism (Azevedo et al., 1991; Azevedo and Portugal Ferreira, 1999, 2006). The third and last phase (<200–3 ka) was characterized by monogenetic effusive and explosive basaltic eruptions, some of them with violent phreatomagmatic activity (Morisseau and Traineau, 1985; Azevedo and Portugal Ferreira, 2006; Andrade et al., 2021a, 2022). These eruptions formed several scoria cones (e.g., Pico do Touro, Marcela, Lomba da Vaca), maars (e.g., Lagoa Funda, Lagoa Negra, Lagoa Comprida), and tuff rings (e.g., Caldeira, Caldeirinha, Lagoa Rasa, Lagoa Branca) throughout the central part of the island (Fig. 1b and c), more rarely in the periphery. These volcanoes emitted several valley-filling lava sequences including those in the Lajes and Fazenda de Santa Cruz valleys. Currently, most of the phreatomagmatic craters are occupied by lakes.

Despite such vigorous periods of volcanism that allowed the island to grow, Flores was also subjected to intense destructive processes, resulting in a complex history of volcanic growth, and destruction (Azevedo et al., 1991; Ramalho et al., 2013; Hildenbrand et al., 2018). Today, the island is characterized by a central depression (500 m asl) – Caldeira das Sete Lagoas – which is the result of a caldera collapse. This depression is filled with the products of the last phase of volcanism (Fig. 1b), indicating that the collapse occurred between the second and the third phases of volcanism, i.e., <200 ka. In the western sector of the island (Fig. 1b), the multi-stage flank collapse of Fajãzinha–Fajã Grande (see Fig. 11a of Ramalho et al., 2013), produced a headwall that exposes the caldera-filling young volcanic sequence abutting against the former caldera wall (Fig. 2a–c). The exact timing of the different stages of this collapse is not known but it has been postulated that the first stage (landslide 1 in Fig. 1b) occurred between 200 ka and the Holocene, and the second stage (landslide 2 in Fig. 1b) is nearly contemporary with the CVS activity, i.e., took place during or after the period between 3660 and 2360 cal yr BP (Andrade et al., 2021a). The short distance between these collapse scars and the CVS vents suggests a relationship between volcanism and the trigger of smaller-scale collapses, as discussed further on in this paper.

The vents and products of the CVS are nested in the northern sector of Sete Lagoas caldera, a relatively flat area presently characterized by extensive peat bogs and water-logged soils (mean annual precipitation ~4600 mm; Secretaria Regional do Ambiente e do Mar, 2012). CVS is stratigraphically above and cuts through the caldera-filling sequence, consisting of a sub-horizontal succession of porous scoria layers, lavas, sediments and (towards the top) phreatomagmatic tuffs, exceeding 250 m in overall thickness (Fig. 2b). This sequence hosts the upper groundwater body of the island, which is composed of several perched aquifers (Azevedo, 1998), drained by numerous perennial springs and waterfalls observable along the exposed Fajãzinha–Fajã Grande collapse scar (Fig. 2c), as well as the perennial lakes that infill Lagoa Negra and Lagoa Comprida craters.

2.1. Flores Holocene volcanism

Although Flores Island did not experience volcanic eruptions in historical time, a period of intense volcanism took place during the Holocene, with at least six eruptions occurring over a time span of ~3000 years (Andrade et al., 2021a, 2022). The most recent volcanic activity of Flores was sourced from Comprida Volcanic System (CVS), previously dated at 3047 cal yr BP (Morisseau and Traineau, 1985) and independently constrained to 3660–2356 cal yr BP by Andrade et al. (2021a). This volcanic system is composed of six phreatomagmatic craters: three maars (Lagoa Negra, Lagoa Comprida, and Lagoa Seca) and three tuff rings (Lagoa Branca, CVS south and east craters; Fig. 1b-c). Preliminary observations of proximal sequences revealed that CVS experienced nearly coeval Strombolian and phreatomagmatic activity (Andrade et al., 2021a). The detailed volcanic sequence, as well as the magnitude of the eruption (or eruptions) are being addressed here for the first time.

The second most recent period of volcanism of the island happened ~200 years prior to the CVS eruption(s) and was characterized by three volcanic events, which were sourced from Funda Volcanic System (FSV) at 3428, 3333, and 3254 cal yr BP (Andrade et al., 2022). The oldest (FVS1) was a small Strombolian eruption, whose products are restricted to the near-vent areas. The second (FVS2) was a violent Strombolian eruption that dispersed tephra across the central and east part of the island. This eruption may have shifted its style, ending with phreatomagmatic explosions that produced dilute pyroclastic density currents (PDCs) and lithic-rich fallout. The third eruption (FVS3) was purely phreatomagmatic and produced dense and dilute PDCs, as well as lithic-rich fallout (Andrade et al., 2022). FVS is currently formed by three (possibly four) craters of phreatomagmatic origin, including Lagoa Funda maar, and Lagoa Rasa and SE crater tuff rings (Fig. 1b).

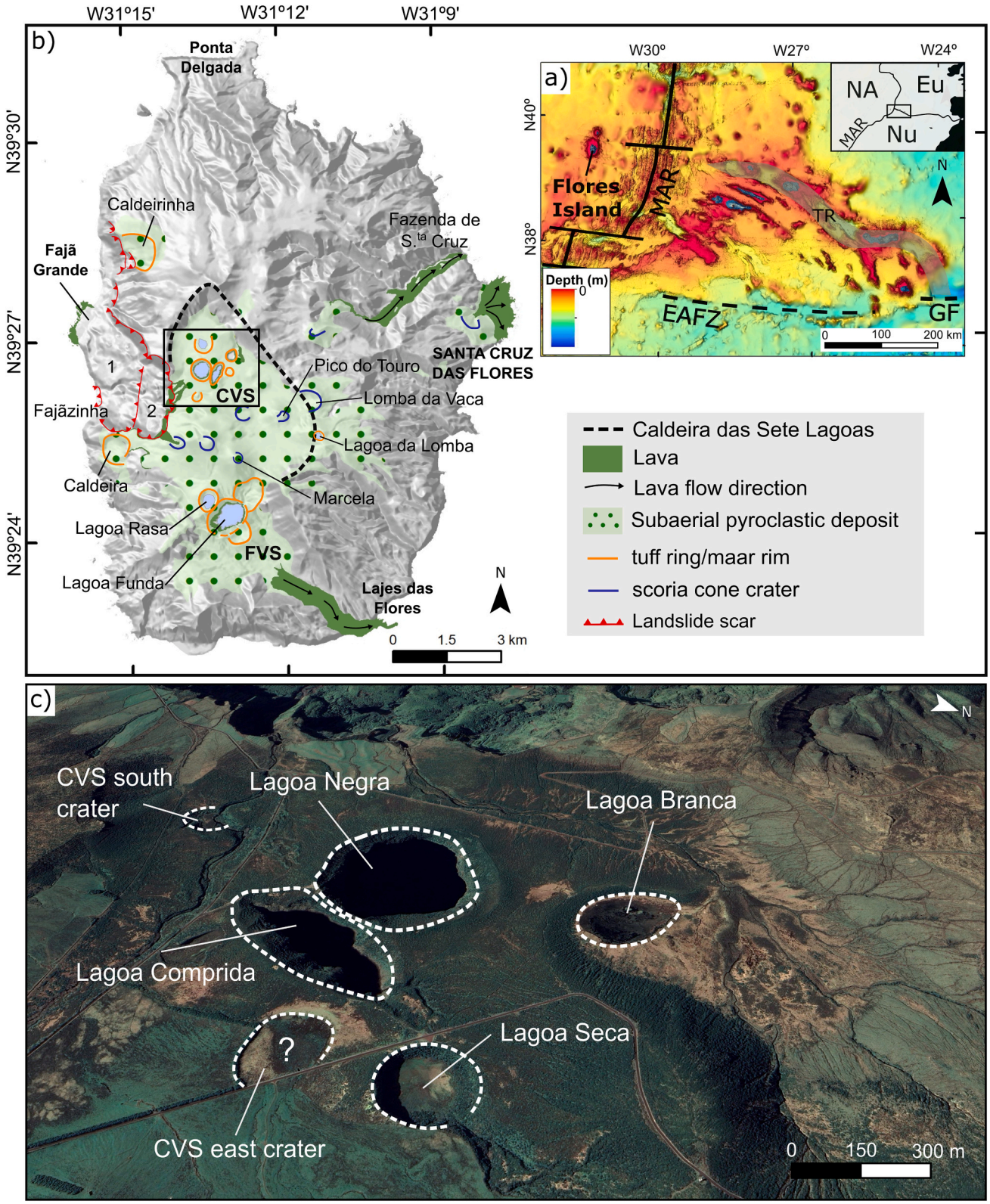

Fig. 1. a) Bathymetric map of the North Atlantic at the Azores triple junction showing the location of Flores Island. MAR – Mid-Atlantic Ridge, EAFZ – East Azores Fracture Zone, GF – Gloria Fault, TR – Terceira Rift. Bathymetry from EMODnet Bathymetry Consortium (2018); Upper right inset depicts the regional setting of the Azores Archipelago at the confluence of the North American (NA), Eurasian (Eu) and Nubian (Nu) lithospheric plates; b) Digital elevation model (hillshade, UTM projection, zone 25 N) of Flores Island showing the volcanic products and the distribution of scoria cones and maars formed during the last phase of volcanism of the island (<200–3 ka). Numbers 1 and 2 (western part of the island) represent, respectively, the first and second main stages of collapse of the Fajãzinha–Fajã Grande multi-stage flank collapse. The island's main town (Santa Cruz das Flores) as well as the other main population centres are indicated; c) Google Earth oblique view showing the different craters of Comprida Volcanic System (CVS).

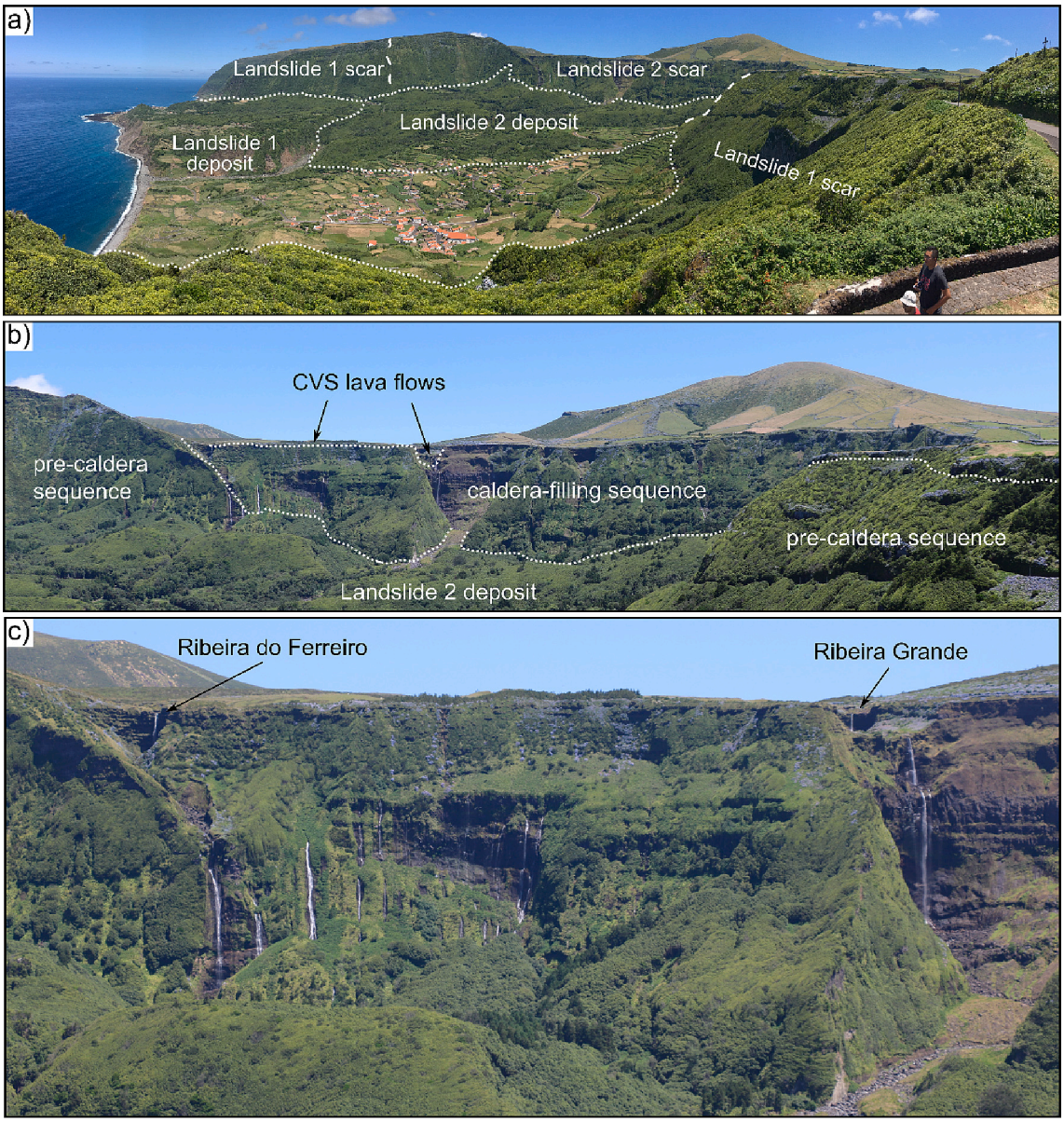

Fig. 2. a) Panoramic view (looking N) of the Fajãzinha–Fajã Grande multi-stage flank collapse, with the deposits and scars of the two main stages identified as landslides 1 and 2 (se also Fig. 1b); b) Detail of landslide 2 headwall, which exposes the contact between the caldera-filling volcano-sedimentary sequence (<200 ka; where the CVS vents and products are installed) and the older pre-caldera volcanic sequence (>320 ka; Hildenbrand et al., 2018); c) Detail of the wall exposing the caldera-filling sequence – note the profusion of water springs and waterfalls draining the perched aquifers of the caldera-filling sequence (photo taken during the dry summer months).

The two older Holocene volcanic events – 6280 and 4990 cal yr BP – were small basaltic eruptions, exclusively magmatic in nature, but their products are not exposed subaerially, being only preserved in Lagoa da Lomba sedimentary record. Their sources are unknown so far, however, Pico do Touro and Marcela scoria cones have been indicated as possible vents (Andrade et al., 2021a). Another possibility is that these eruptions may have been sourced from older vents that are now covered/destroyed by the products of the recent eruptions of FVS and CVS.

3. Methods

3.1. Fieldwork

The volcanostratigraphy of CVS was studied during two field work campaigns that took place in the summers of 2019 and 2020. In addition to geological field mapping, a total of 164 stratigraphic sections were studied in detail and their deposits systematically described in terms of thickness, grain size, components, texture, internal structures, and spatial distribution. Coordinates of field stations are listed in Supplementary material 1. The maximum clast size of tephra fall deposits was obtained by measuring the length of the major axis of the five largest juvenile and lithic clasts and averaging the values. Paleosols, erosion surfaces and unconformities were used to recognize the limits of the deposits and to identify possible time-breaks in the volcanic record.

Tephra samples for glass geochemical analysis were collected at the most representative sequences across the study area. Additionally, organic-rich paleosols underlying pyroclastic deposits were collected for radiocarbon dating. The stratigraphical and morphological relationships between the CVS volcanic sequences and the collapse deposits of the Fajãzinha-Fajã Grande gravitational structure (Fig. 2) were also investigated in the field.

3.2. Physical parameters

The volume of tephra fall deposits was calculated based on the isopach map using the method of Pyle (1989) modified by Fierstein and Nathenson (1992). Tephra bulk densities were determined at the laboratories of Faculdade de Ciências da Universidade de Lisboa – FCUL (Portugal) – by weighting five representative samples in beakers with known volume. Erupted mass was determined based on the minimum and maximum values obtained for the tephra densities (844 to 915 kg/m^3). The magnitude of the eruption was calculated following Pyle (2000). Tephra volume was converted to dense rock equivalent (DRE) volume considering the tephra bulk densities and a trachybasalt magma density of 2800 kg/m^3 (Pimentel et al., 2016).

3.3. Geochemistry

Twenty tephra samples were washed, dried, manually crushed and sieved at FCUL. The 63–125 μm (4-3Φ) fraction of each sample was mounted into acrylic tablets with epoxy resin at GEOMAR Helmholtz Centre for Ocean Research, Kiel (Germany). The tablets were polished and carbon-coated for electron microprobe (EMP) analysis. Fifteen glass shards from each sample were analysed for major and minor elements

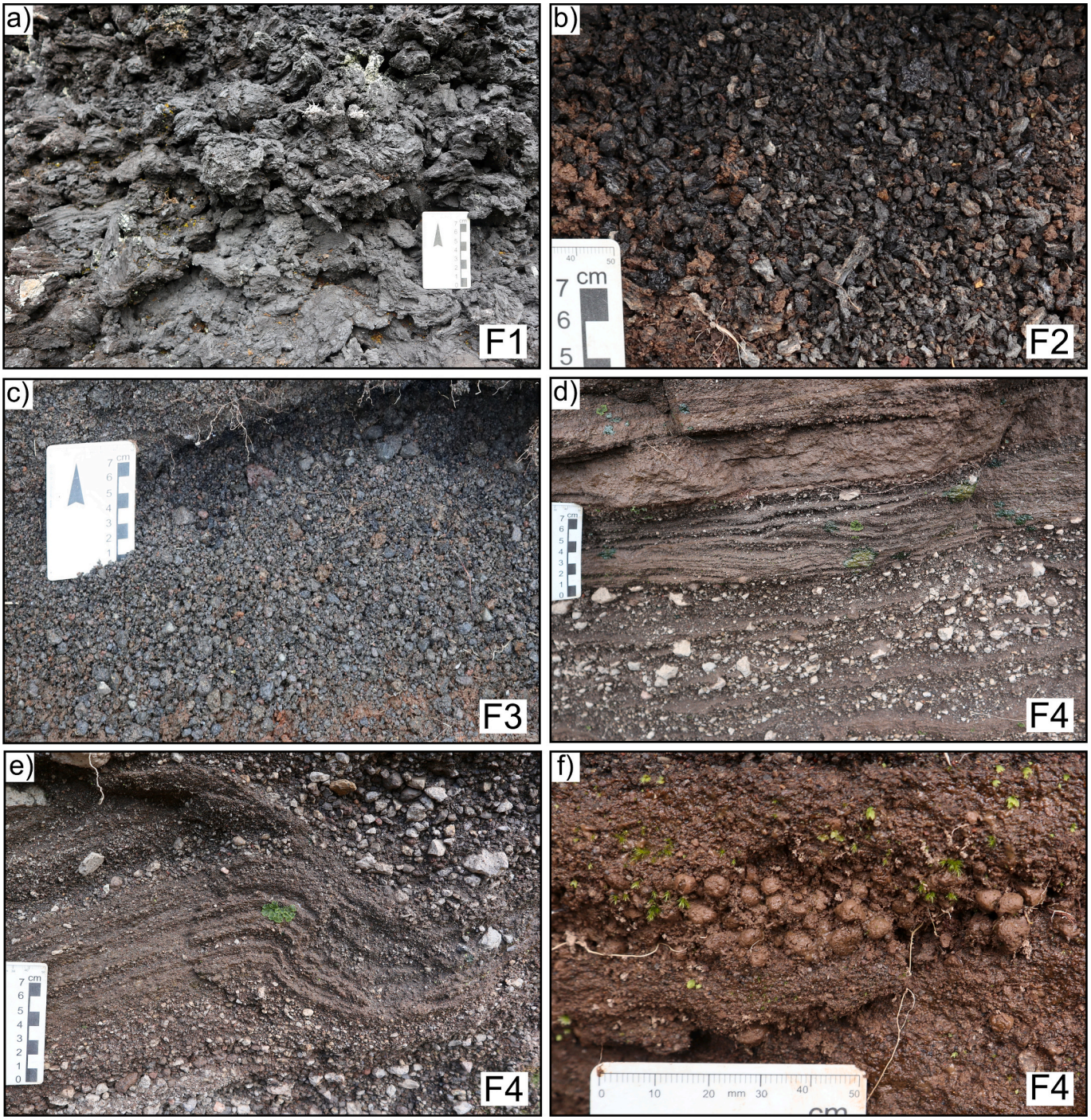

Fig. 3. CVS lithofacies: a) spatter; b) massive fluidal-shaped scoria lapilli/ash; c) massive lithic-rich lapilli/ash; d) bedded lithic-rich ash and lapilli, showing the parallel alternation between fine ash beds and lapilli beds; e) bedded lithic-rich ash and lapilli, showing cross- and wavy-stratification; f) bedded lithic-rich ash and lapilli, with accretionary lapilli.

using a JEOL JXA 8200 wavelength dispersive EMP following the methods by Kutterolf et al. (2011).

EMP analyses were calibrated based on international standards. A 10 μm electron beam and 6 nA beam current were used to minimize sodium loss. Oxide concentrations were determined using the ZAF correction. To ensure accuracy of the analyses measurements were monitored using Lipari obsidian (Lipari rhyolite; Hunt and Hill, 2001) and Smithsonian basaltic standard VGA99 (Makaopuhi Lava Lake, Hawaii; Jarosewich et al., 1980), with two measurements on each standard after every sixty glass shard measurements. Standard deviations are <0.5% for major elements and < 10% for minor elements.

All the analyses were normalized to 100 wt% to eliminate effects of variable post-depositional hydration and minor deviations in the focus of the electron beam. Analysis with totals below 97 wt% were not considered. The acceptable analyses include a total of 170 glass shards, which were statistically processed to characterize the elemental compositions of each sample. Major and minor element data and their corresponding errors are listed in Supplementary material 2 and Supplementary material 3, respectively.

3.4. Radiocarbon dating

A total of four paleosols and one charcoal fragment embedded in a paleosol were analysed at the Radiochronology Laboratory of the Centre d'Études Nordiques, University of Laval (Canada) for Accelerated Mass Spectrometer (AMS) radiocarbon dating. To remove inorganic carbon from the samples, paleosols were subjected to a HCl – NaOH – HCl pretreatment. The reported conventional ^{14}C ages were calibrated to "cal yr BP" using the CALIB 8.2 software and the IntCal20 calibration curve (Stuiver et al., 1993). Due to the calibration model uncertainties, ages were rounded to tens of years.

4. Results

4.1. Characterization of CVS lithofacies

Based on their characteristics (i.e., grain size, components, textures, and internal features), the different pyroclastic deposits of CVS were divided into four main volcanic lithofacies, numbered from F1 to F4 (Fig. 3):

Spatter (F1): black/dark grey blobs of lava or bombs (up to 25 cm), with well-preserved fluidal shapes, very vesicular, and containing large (up to 3 cm) crystals of olivine and plagioclase. Occasionally, lithic blocks (up to 20 cm), syenite xenoliths (~3 cm), and loose olivine crystals (~1 mm) are present. In most outcrops, spatter fragments are stacked and agglutinated (welded spatter), but in a small number of sites spatter clasts are supported by a matrix of scoria lapilli and ash. This facies is limited to the proximal areas of the Lagoa Comprida and Lagoa Negra craters.

Massive scoria lapilli/ash (F2): dark grey medium lapilli to coarse ash with well-preserved fluidal and scoriaceous textures, clast-supported and relatively well-sorted. Juvenile clasts (scoria) are predominant (varying from >50% up to ~100%), with variable amounts of lithic clasts (including rare syenite xenoliths), loose olivine and plagioclase crystals dispersed within the unit(s); sometimes containing large juvenile bombs (up to 11 cm). This facies is ubiquitous in the CVS area. Its thickness varies from 44 to 13 cm in proximal areas, with consistent thinning and fining (grain size) with distance from the source. Conversely, sorting increases with distance. In the proximities of CVS, these deposits are buried by more recent products and usually well-preserved (e.g., FL105MA; Supplementary Fig. 1a). In the southeast sector, they occur on top of older volcanic sequences, where they are more exposed to weathering and erosion, and usually intensively palagonitized (e.g., FL53MA, Supplementary Fig. 1b).

Massive lithic-rich lapilli/ash (F3): grey/dark grey medium lapilli to fine ash, blocky particles, clast-supported and relatively well-sorted. Lithic clasts are predominant (varying from >50% up to ~100%), with subordinate amounts of juvenile clasts, and loose olivine and plagioclase crystals; sometimes containing large lithic blocks (up to 20 cm). This facies is limited to the areas located to the east of CVS. Its thickness (25 cm maximum thickness) and grain size decrease with distance from the source area, while the sorting increases.

Bedded lithic-rich ash and lapilli (F4): grey/brownish alternating lithic-rich fine ash beds and lithic-rich medium to fine lapilli beds. The fine ash beds contain dispersed lapilli-sized lithic clasts, many show cross- and wavy-stratification and sometimes bomb-sag structures and accretionary lapilli. The lapilli beds are usually clast-supported and well-sorted. Large lithic blocks (up to 90 cm) are typically present. This facies is mainly present is the surroundings of CVS. The thickness and grain size of the deposits vary depending on the outcrop location relatively to the source area, being thicker and coarser in the north and west areas (Fajã Grande, see Fig. 1b and 2) of the CVS. Although absent to the east, this facies is also present in the south and southwest, but its thickness decreases rapidly with distance from the source and the well-defined internal stratification becomes diffuse (e.g., outcrop FL106MA; Supplementary Fig. 1c). These deposits almost disappear ~3 km away from the centre of CVS, where only an inconspicuous and altered ash bed (up to 27 cm) with dispersed lithic lapilli is present (FL86MA; Supplementary Fig. 1d).

4.2. Description of volcanic sequences

CVS sequences are considerably different depending on the location of the outcrop in relation to the source area. Accordingly, a total of 17 volcanic sequences were selected as the most representative to show the spatial distribution and stratigraphic relations of the different facies.

Despite the dense vegetation of Flores, an abandoned quarry provided a good exposure of the southeast flank of Lagoa Comprida volcanic edifice (outcrop FL17MA; Fig. 4a and b). The exposure starts with a thick (>4 m) sequence of spatter accumulation (F1; Fig. 4b), containing large bombs (up to 25 cm) and occasional lithic blocks (up to 20 cm). Accidental lithics become more frequent and spatter grain size decreases towards the top of the unit, with spatter being gradually replaced by massive scoria lapilli (F2). On top of the scoria lapilli unit (Fig. 4a) is a 20-cm-thick layer of large lithic blocks (up to 20 cm) supported by a coarse ash matrix (F3), which, in turn, is overlapped by a thin ~3-cm-thick) massive scoriaceous ash layer (F2). The volcanic sequence ends with a thick (170 cm) bedded lithic-rich ash and lapilli deposit, of intercalating fine ash beds, with cross- and wavy-stratification, and fine to medium lapilli beds (F4). Large lithic blocks (up to 20 cm) are dispersed throughout this unit, especially in the upper part, sometimes forming bomb-sag structures. This bedded sequence is inclined, draping over the flank of the volcanic edifice (Fig. 4a).

A similar sequence of spatter (F1), massive scoria lapilli (F2) and bedded lithic-rich ash and lapilli (F4) is observed southwest of Lagoa Negra maar (outcrop FL104MA; Fig. 4c). In this location, the spatter accumulation is >50 cm thick and spatter clasts are embedded in a scoriaceous lapilli-ash matrix with rare lithics. Spatter bombs are smaller (up to 10 cm) and less vesicular than those from outcrop FL17MA, resulting in slightly denser and blocky textures (Fig. 4c). Towards the top of the deposit is a gradual transition from spatter to scoria lapilli, accompanied by an increase of lithic clasts. The massive scoria lapilli unit is 42 cm thick and contains abundant juvenile bombs (up to 11 cm). The upper bedded lithic-rich ash and lapilli sequence is >3 m thick and contains large lithic blocks (up to 90 cm).

Outcrop FL18MA (located ~500 m southeast from the rim of Lagoa Comprida; Fig. 4d) is the site where the CVS sequence is most complete, and therefore, one of the best exposures to constrain its tephrostratigraphy. In this location, two volcanic sequences can be distinguished, both limited at the base by erosive surfaces and dark, well-developed paleosols rich in organic matter. The lower volcanic sequence is formed by an intensively palagonitized scoria lapilli unit (~20 cm

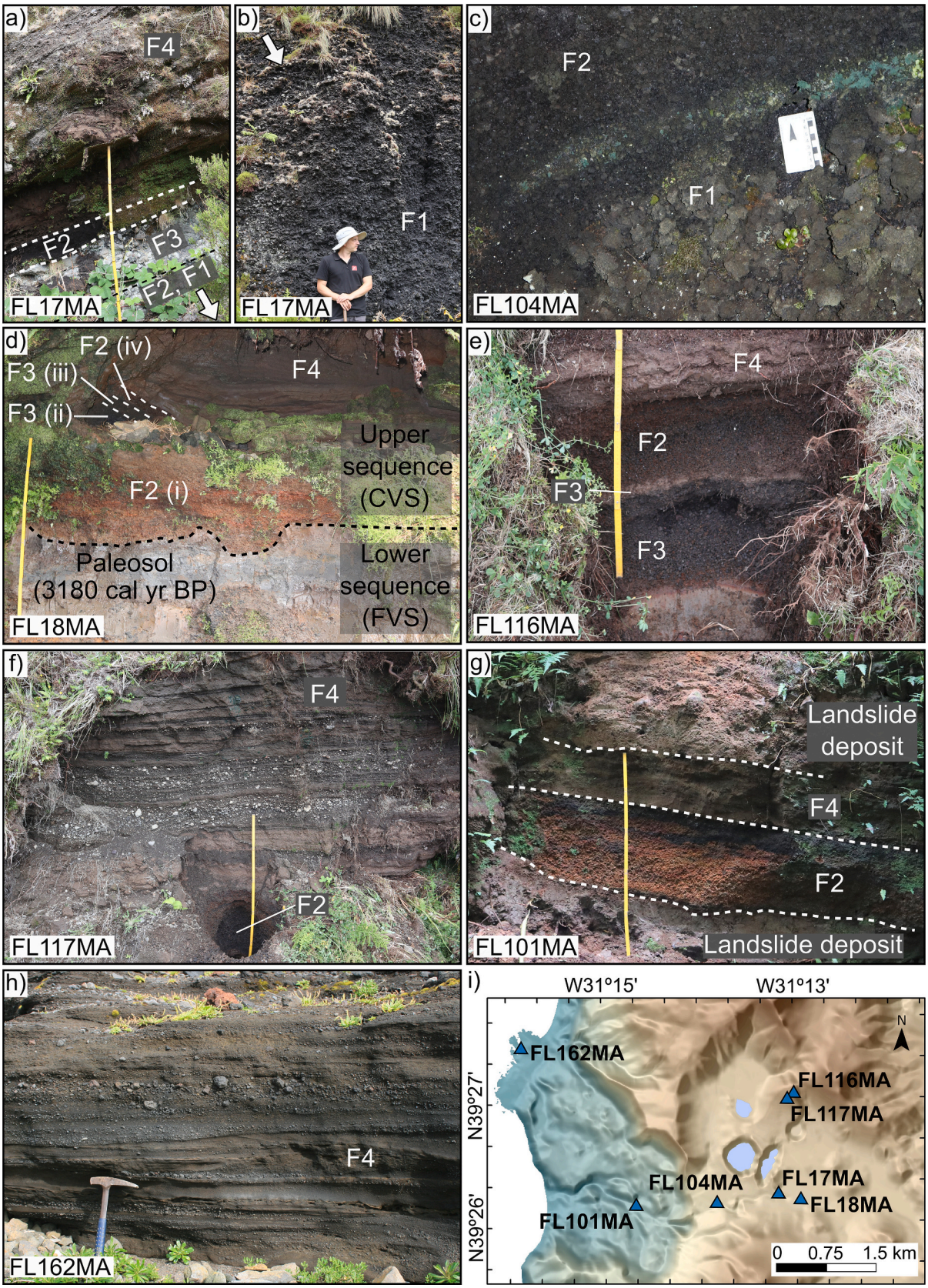

(caption on next page)

Fig. 4. Field photographs of selected CVS sequences: a) and b) proximal sequence located at the rim of Lagoa Comprida maar (outcrop FL17MA) showing the transition from spatter and massive scoria lapilli deposits (F1 and F2) to massive and bedded lithic-rich deposits (F3 and F4); c) outcrop FL104MA, located close to the rim of Lagoa Negra maar, showing spatter fragments in a coarse ash to fine lapilli matrix (F1) overlapped by massive scoria lapilli (F2); d) outcrop FL18MA showing the complete CVS sequence overlaying a paleosol dated at 3180 cal yr BP. The CVS sequence is overlapping the older FVS sequence and it consists of (from the base to top) massive scoria lapilli (F2), lithic-rich lapilli and ash (F3), massive scoria lapilli (F2), and bedded lithic-rich ash and lapilli (F4); e) outcrop FL116MA, showing two massive beds separated by a thin lithic-rich ash layer (F3), the lower is a lithic-rich lapilli bed (F3), and the upper a scoria lapilli bed (F2). These units are overlapped by a bedded lithic-rich sequence of ash with cross- and wavy-stratification, intercalated with lapilli beds/lenses (F4); f) outcrop FL117MA showing a massive scoria lapilli deposit (F2) at the base, overlapped by a thick sequence of alternated lithic-rich fine ash and lapilli (F4), with the finer layers showing cross- and wavy-stratification, as well as accretionary lapilli; g) outcrop FL101MA showing the CVS deposits (F2 and F4) in between two massive landslide deposits; h) outcrop FL162MA, located at Fajã Grande (~4 km from the CVS vents), showing a thick bedded lithic-rich sequence of ash layers with cross- and wavy-stratification, intercalated with lapilli beds containing blocks (up to 10 cm) and a significant amount of juvenile clasts; i) digital elevation model (hillshade) showing the location of the referred outcrops.

thick), which is overlain by a thin (~10 cm) layer of ash containing lenses of fine lithic lapilli. Although the weathering of the deposits prevents a good observation of its internal features, the sequence is consistent with the descriptions made by Andrade et al. (2021a, 2022) for the stratigraphic succession of FVS. The upper volcanic sequence comprises alternating massive scoria lapilli/ash and massive lithic-rich lapilli/ash deposits (Fig. 4d and Supplementary Fig. 2a). From the base to the top the sequence consists of i) 74-cm-thick scoria lapilli (F2). Although slightly palagonitized, the juvenile clasts show well-preserved fluidal and vesicular shapes. Numerous lithics and loose olivine crystals are present; ii) 20-cm-thick lithic-rich medium to fine lapilli (F3), containing rare juveniles; iii) 9-cm-thick lithic-rich coarse ash to fine lapilli (F3), containing several juveniles; iv) 8-cm-thick scoria lapilli (F2), containing loose olivine crystals and rare lithics. This pattern of scoria – lithic-rich – scoria deposits is consistent across the area to the east of CVS (e.g., outcrops FL158MA and FL127MA; Supplementary Fig. 2b and c). The volcanic sequence ends with a 1-m-thick bedded lithic-rich ash and lapilli deposit (F4; Fig. 4d).

In the area north of CVS, two massive beds crop out separated by a thin (~2 cm) lithic-rich ash layer (e.g., outcrop FL116MA; Fig. 4e). The lower bed (~23 cm thick) is composed of medium to fine lapilli, almost exclusively lithic clasts (F3), but also loose rare olivine crystals and juveniles, the latter becoming more frequent in the upper part of the unit. The base is limited by an erosive surface. The upper massive bed (~20 cm) is mainly composed of scoria lapilli (F2), abundant loose olivine crystals, lithic clasts, and rare syenite xenoliths. The grain size of the juvenile particles decreases towards the top of the unit (from medium to fine lapilli) and the lithics become more abundant. This massive scoria unit (F2) is overlapped by a well-bedded lithic-rich sequence (up to 150-cm-thick) of alternating fine ash layers and fine to medium lapilli and coarse ash layers (F4; e.g., outcrops FL117MA; Fig. 4f). The fine ash layers usually show cross- and wavy-stratification, bomb-sag structures, and accretionary lapilli (up to 1 cm in diameter). The coarser layers are essentially composed of lithic lapilli particles, sometimes containing large lithic blocks (up to 26 cm). These coarser beds are generally well-sorted but the grain size varies vertically along the deposit from coarse ash to coarse lapilli (Supplementary Fig. 2d).

CVS pyroclastic deposits are, in most locations, the youngest unit that crops out and, consequently, its top is usually altered and/or eroded. An exception is the lower area located to the west of Sete Lagoas caldera (within the Fajãzinha-Fajã Grande landslide structure), where the massive scoria lapilli/ash (F2) and the bedded lithic-rich ash and lapilli sequence (F4) are between two massive landslide deposits (with blocks >1 m) e.g., outcrop FL101MA (Fig. 4g).

At Fajã Grande (e.g., outcrop FL162MA; Fig. 4h; Fig. 5), the bedded lithic-rich ash and lapilli sequence (F4) does not overlap the massive scoria lapilli/ash (F2) or lithic-rich lapilli/ash (F3) deposits (which are not preserved in the area) but instead lies on top of the A'a lavas forming the Fajã Grande lava delta, filling the spaces between the A'a spines and clinker of these lavas. Despite being ~4 km away from the CVS vents, at this site, the bedded lithic-rich sequence (F4) is ~115 cm thick. The fine ash layers show cross-stratification and sometimes lenses of lithic lapilli and blocks (up to 10 cm), while the coarse ash/fine lapilli layers are very heterogeneous, containing mainly lithics but also juvenile particles, occasionally rounded, and loose olivine crystals (Fig. 4h). In some areas, the bedded lithic-rich sequence is overlain by a debris flow deposit (derived from the latest landslides) containing large blocks (>1 m; see Fig. 5).

4.3. Geological mapping and geomorphological analysis

Detailed geological mapping and geomorphological analysis of the area around CVS shows that this volcanic system forms a positive relief (Fig. 5a), up to 60 m above the pre-existing volcanic basement, which is exposed along the crater walls of Lagoa Negra, Lagoa Comprida, and Lagoa Seca maars. Moreover, exposures on these crater walls also confirm (in the case of Lagoa Negra and Comprida) that the first products to be erupted by the CVS correspond to magmatic lithofacies F1 and F2 (spatter and scoria lapilli/ash), with lithofacies F3 and F4 (massive and bedded lithic-rich lapilli/ash) resting above these, with their sedimentary structure being in direct link with the volcanic constructive morphology observable today. Mapping revealed the presence of a series of lava flow lobes (exhibiting leveed channels on top) extending to the west of the Lagoa Negra/Lagoa Comprida constructional relief (Fig. 5b), down to the cliff edge of the Fajãzinha–Fajã Grande youngest collapse scar (landslide 2 in Fig. 1b, Fig. 2a and Fig. 5c); the southernmost of these lobes is also seen cascading and partially infilling the upper reaches of the Ribeira Grande valley above the cliff (see Fig. 5b and c).

Mapping also revealed that the lava delta of Fajã Grande was formed by flows that partially infilled and drained from a valley cut into the older Fajãzinha-Fajã Grande landslide deposits (Fig. 1b and Fig. 5c-d), resting against the sea cliffs that were carved into these landslide deposits (Fig. 5d). These lavas, however, cannot be traced continuously back to their source, as they are covered by the deposits of the second main stage of collapse (landslide 2 in Fig. 1b, Fig. 2a and Fig. 5c).

4.4. Radiocarbon ages

Four paleosol and one charcoal (embedded in a paleosol) samples from four different key-sequences were dated (Table 1) to constrain the age of CVS activity. CVS pyroclastic deposits are, in most cases, overlapping an older volcanic sequence, that records at least three eruptions dated between 3430 and 3250 cal yr BP, associated with FVS (Andrade et al., 2021a, 2022).

At outcrop FL18MA, well-developed paleosols are present at the base of both FVS and CVS sequences. The paleosol below the FVS sequence was dated at 3935 cal yr BP, while the paleosol at the base of CVS sequence was dated at 3180 cal yr BP (Fig. 4d; Table 1). At outcrops FL127MA and FL37MA, the limit between the two volcanic sequences is marked by an erosive surface, without the presence of paleosols (Supplementary Fig. 2c and e). Nevertheless, a paleosol and a charcoal fragment at the base of the FVS sequence were dated to ensure consistency in the stratigraphy. The paleosol from outcrop FL127MA was dated at 3920 cal yr BP, an age similar to the one obtained for the paleosol below FVS deposits at outcrop FL18MA, and the charcoal from outcrop FL37MA was dated at 3280 cal yr BP (Table 1), an age that is

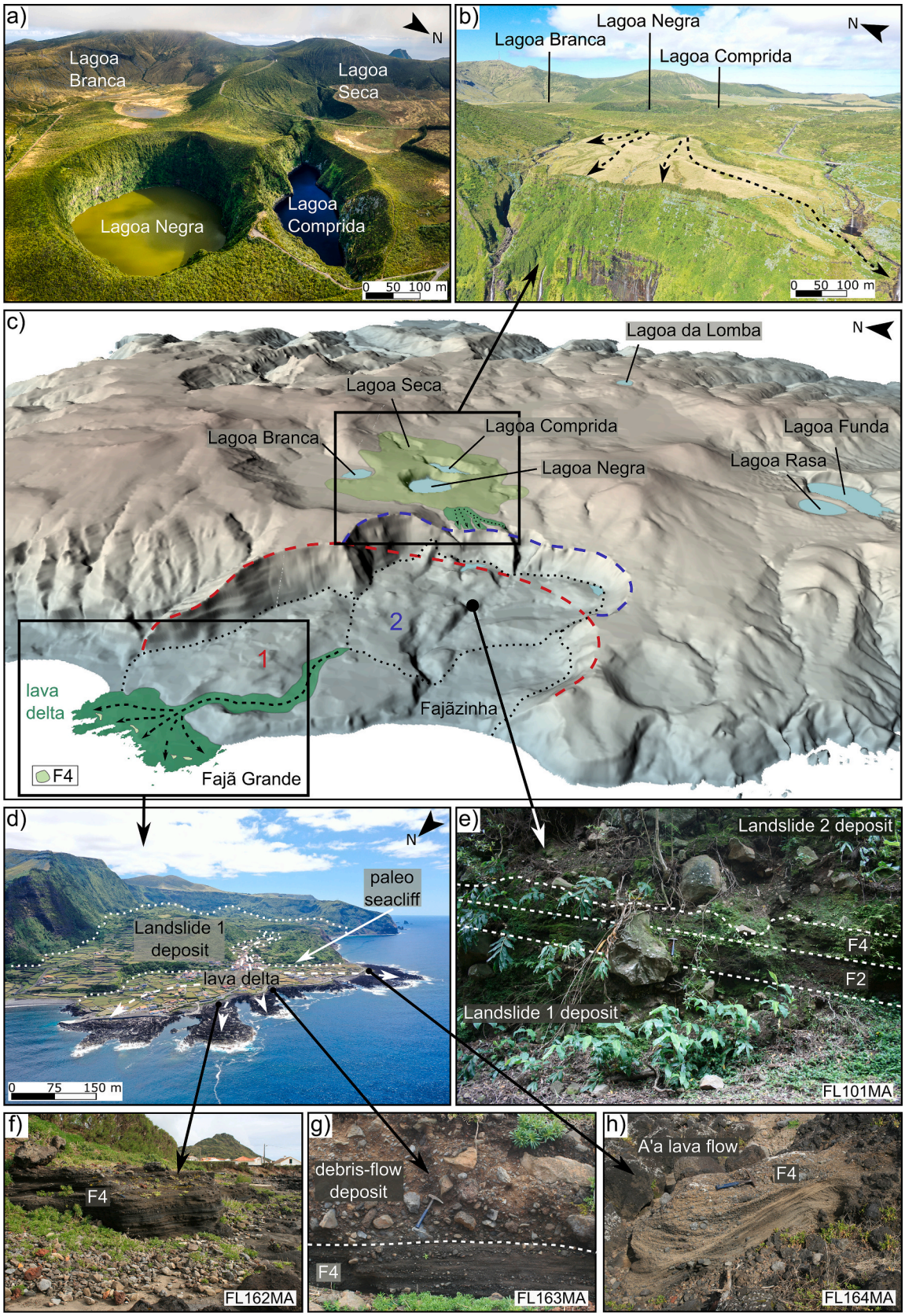

(caption on next page)

Fig. 5. Spatial relations of CVS craters and volcanic facies: a) Oblique aerial view (looking north) of the CVS main craters (Lagoa Seca, Lagoa Branca, Lagoa Comprida, and Lagoa Negra). Photograph by Bruno Ázera; b) Oblique aerial view (looking east) of CVS, showing the lava flows that extruded during the effusive episode, which are cut by the scar of the most recent landslide 2 (see next subfigure) that affected the western margin of Sete Lagoas caldera; c) 3D digital elevation model (looking east-northeast) of Flores, showing the CVS craters and respective lavas. Note how the young lava delta of Fajã Grande – which drained down a valley carved into the older landslide 1 – was probably fed from CVS; the link between the proximal and distal lavas was most likely severed by the younger landslide 2; d) Oblique aerial view (looking south-southeast) of the Fajã Grande lava delta; e) Outcrop near the confluence of Ribeira do Ferreiro and Ribeira Grande streams, which displays a primary pyroclastic sequence between the deposits of the two major landslides, attesting to the occurrence of volcanic activity between the older and younger landslides; f) outcrop FL162MA showing the bedded lithic-rich ash and lapilli sequence (F4) at Fajã Grande; g) outcrop FL163MA showing the bedded lithic-rich ash and lapilli deposit (F4) overlapped by a landslide deposit (debris flow) at Fajã Grande; h) outcrop FL164MA showing the bedded lithic-rich ash and lapilli deposit (F4) on top of the A'a lavas at Fajã Grande.

Table 1
AMS radiocarbon dates and respective calibrated ages obtained at different volcanic sequences.

Sample ID	Location	Lab #	Type of Sample	$D^{13}C$ (‰)	$F^{14}C$	±	$D^{14}C$ (‰)	±	^{14}C age (BP)	±	Median probability (cal yr BP)	2σ (cal yr BP)
FL18MA-1	N39°26′12.37” W31°12′57.24”	ULA-9374	paleosol	−27.3	0.637	0.001	−363	1	3625	15	3935	-58/+48
FL18MA-2	N39°26′12.37” W31°12′57.24”	ULA-9369	paleosol	−25.3	0.689	0.001	−311	1.2	2995	15	3183	-43/+50
FL37MA-3	N39°25′41.74” W31°11′15.86”	ULA-9357	charcoal	−28.7	0.684	0.001	−316.2	1.1	3055	15	3276	+6/+64
FL114MA-1	N39°27′27.54” W31°12′46.30”	ULA-9354	paleosol	−27.3	0.611	0.001	−389.3	1.1	3960	15	4428	-25/+18
FL127MA-1	N39°25′25.82” W31°10′22.55”	ULA-9371	paleosol	−26.4	0.638	0.001	−362.2	1	3615	15	3924	-53/+55

compatible with the start of FVS2 eruption (Andrade et al., 2022). The charcoal fragment was recovered from the upper part of the paleosol, at the contact with the scoria deposit from FVS2 eruption.

The FVS sequence is not present in the outcrops located to the north of CVS. In this area, CVS is covering older and very altered volcanic products whose source is unknown. A paleosol at the base of CVS sequence (outcrop FL114MA) was dated at 4430 cal yr BP (Table 1).

4.5. Geochemistry of CVS tephra

Due to the lack of juveniles in the bedded lithic-rich ash and lapilli sequences, the geochemistry of CVS products is restricted to analyses of the massive scoria lapilli/ash beds (F2). Glass shard compositions are homogeneous, with 45–48 wt% of SiO_2 and 4–7 wt% of total alkalis ($Na_2O + K_2O$). Most of the analyses cluster in the trachybasalt compositional field, although a few plot in the basalt and tephrite basanite fields (Fig. 6). Variation diagrams of selected major elements vs. CaO show a single geochemical population, which overlaps the previously defined geochemical group 3 associated with CVS (Andrade et al., 2021a, 2022) (Fig. 6b-f). Overall, CVS tephras are geochemically less evolved (lower SiO_2 and higher MgO contents) than the products of the older FVS eruptions.

5. Discussion

5.1. Interpretation of lithofacies

Spatter (F1): The spatter in the vicinities of Lagoa Comprida and Lagoa Negra maars is interpreted as the proximal product of Hawaiian-style lava fountaining, revealing that transport by ballistic trajectory played an important role in proximal areas. These deposits attest to the construction of spatter ramparts, possibly along an eruptive fissure.

Massive scoria lapilli/ash (F2): Based on the characteristics of the deposits such as consistent thinning and fining with distance from the source, the generally good sorting, the clast-supported nature, predominant juvenile content, and pristine scoriaceous textures/morphologies of the juvenile clasts, these are interpreted as scoria fall deposits resulting from magmatic Strombolian explosions.

Massive lithic-rich lapilli/ash (F3): Based on thinning and fining of the deposits with increasing distance from the source, the generally good sorting, clast-supported nature, and predominant lithic content, these are interpreted as lithic fall deposits, that resulted from phreatomagmatic explosions, associated with the excavation of the CVS maars. The occasional presence of large lithic blocks reveals that transport by ballistic trajectory was important in proximal areas.

Bedded lithic-rich ash and lapilli (F4): Based on the characteristics of these deposits, such as thin-bedding, lithic-rich nature, abundance of fine ash, presence of accretionary lapilli, and wavy- and cross-stratification, they are interpreted as resulting from simultaneous deposition of ash and lapilli fallout and dilute PDCs (surges) associated with phreatomagmatic activity. The presence of lithic blocks and bomb-sag structures provide evidence for ballistic ejecta in proximal areas.

5.2. Eruptive history of CVS

The eruptive history of CVS is here reconstructed by combining volcano- and tephrostratigraphy with geochronology, glass geochemistry, and geomorphology (Fig. 7). The base of CVS pyroclastic sequence is usually recognized by the presence of erosive surfaces and/or paleosols. In the central part of the island, i.e., in Sete Lagoas caldera, CVS tephras are usually unconformably overlying the volcanic products of FVS (Fig. 7). Glass compositions of CVS tephras are clearly distinct from the compositions of FVS products (Andrade et al., 2022) and fit well with the geochemical group 3 of Lagoa da Lomba lacustrine record (Andrade et al., 2021a). CVS glass compositional data corroborate the general geochemical trend observed by Andrade et al. (2021a, 2022), in which the volcanic products tend to become less evolved as one moves up in the recent stratigraphy of Flores (Fig. 6).

Despite the different volcanic facies and number of craters (at least 5), no paleosols or noticeable unconformities were observed within the CVS pyroclastic sequence (Fig. 7). Accordingly, and considering that only a few decades would be enough to develop a soil in a humid environment like the one of Flores Island (Andrade et al., 2022), we infer that all CVS products were erupted during a single eruptive episode, which occurred in a short period of time that may have lasted only a few days or a few months, as typically seen at Hawaiian-Strombolian (Taddeucci et al., 2015) and maar eruptions (Ort et al., 2018; Ball, 2022).

Our new radiocarbon ages are consistent with the age intervals proposed by Morisseau and Traineau (1985) and Andrade et al. (2021a), suggesting that the CVS eruption occurred at least approx. 3180 cal yr

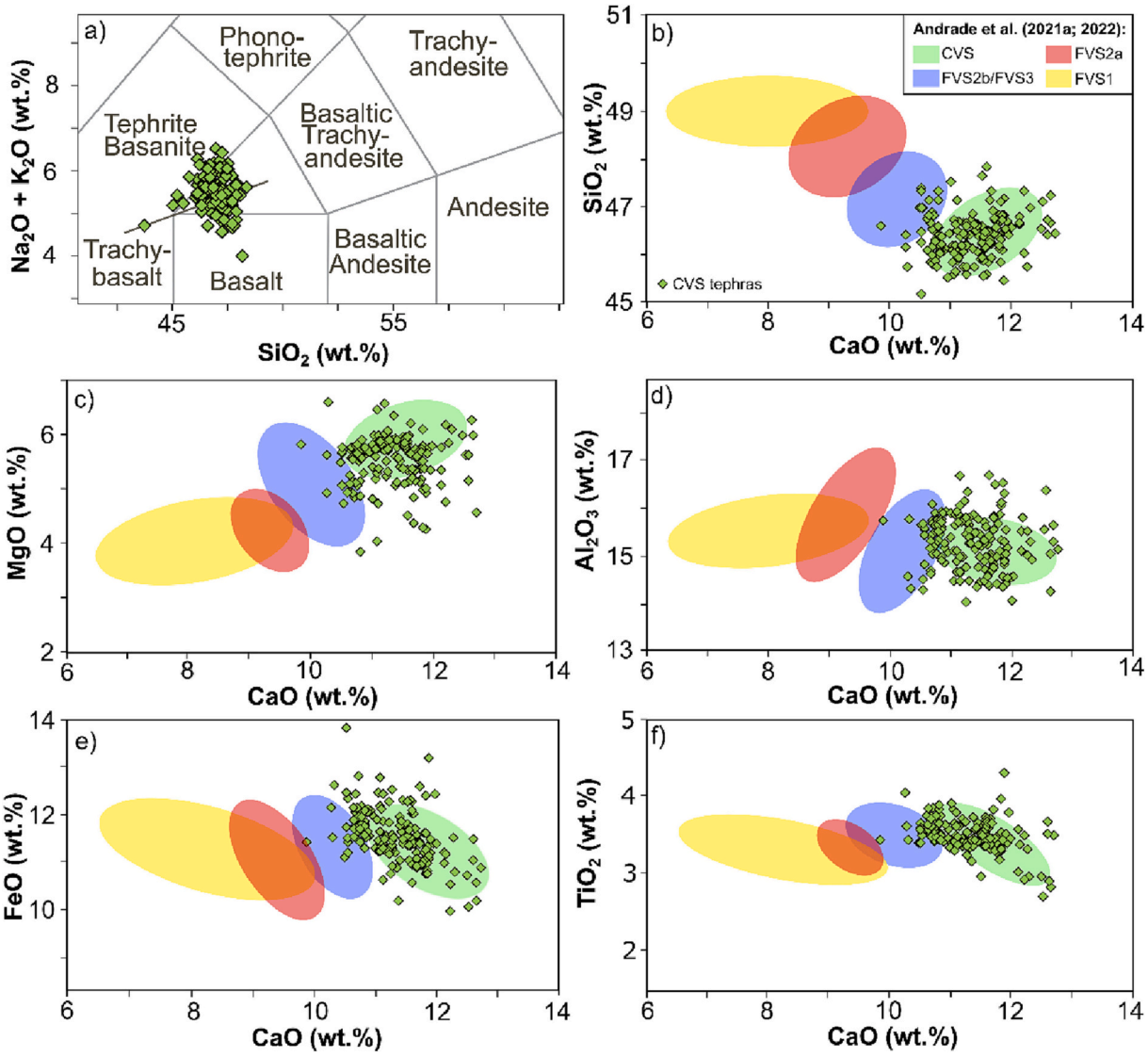

Fig. 6. a) Total alkalis vs silica (TAS) diagram (LeBas et al., 1986) for the classification of glass analysis from CVS massive scoria lapilli/ash beds (F2). Compositions cluster around the trachybasalt compositional field; b-f) variation diagrams of major elements (wt%) vs. CaO (wt%). Shaded coloured fields represent geochemical groups defined by Andrade et al. (2021a, 2022), associated with FVS and CVS juvenile products. Glass compositions are normalized to 100 wt% volatile free.

BP, ~70 years after the previous eruptive episode on the island (FVS3), which was sourced from FVS (Fig. 8). Although the upper limit of the FVS3 eruption age envelope overlaps the lower limit of the age of CVS eruption, suggesting that these eruptions may have been contemporaneous (Fig. 8), the erosive surfaces and especially the presence of paleosols separating the FVS and CVS pyroclastic sequences (e.g., outcrop FL18MA; Fig. 4d) attest to a time break between the two volcanic episodes, possibly of several decades. This suggests that the onset of volcanic activity at CVS most likely did not occur on the lower limit of the uncertainty envelope of the 3183 (−43/+50) cal yr BP age (Fig. 8).

Although complex and spatially variable, the stratigraphy of CVS is coherent, with volcanic sequences showing a general trend varying from spatter/scoriae to lithic-rich deposits, indicating that magmatic activity was dominant in the early stages of CVS eruption and phreatomagmatism became prevalent in the final stages (Fig. 7), as previously reported by Morisseau and Traineau (1985), Azevedo and Portugal Ferreira (2006), and Andrade et al. (2021a, 2022).

The initial phase started with Hawaiian-style lava fountaining, followed by Strombolian-style explosions. It was responsible for the construction of Lagoa Comprida spatter rampart exposed at the quarry (field site FL17MA; Fig. 4b) and crater walls, as well as by another volcanic edifice, probably a small scoria cone, at the site where Lagoa Negra now stands, as attested by the still noticeable positive relief (>60 m above pre-existing topography) in this area.

The Lagoa Negra scoria cone and the Lagoa Comprida spatter rampart (or a single volcanic edifice with at least two vents) must have been erupting at the same time, or alternately, producing a thick sequence of spatter accumulation (F1) in the proximal areas, but also lapilli-sized tephras that were dispersed across the central part of the island (F2). Additionally, geomorphological and stratigraphic evidence suggest that this eruptive phase was also characterized by an important effusive episode, flowing to the west, and which probably formed the lava delta of Fajã Grande (Fig. 5) at the coast. This effusive episode is attested by the presence of lava flow lobes that radiate from the base of Lagoa Negra cone and extend westwards to the landslide scar, and which partially infilled the upper reaches of the Ribeira Grande valley, before reaching the main waterfall. We also infer that these lava flow lobes were once in continuity with the lavas that drained through the old valley carved into the landslide 1 deposit that led to Fajã Grande, to form the youthful coastal lava delta at this locality. This connection is now severed by the scar and deposits of the youngest stage of collapse of the Fajãzinha-Fajã Grande slump (landslide 2). Also, the presence of phreatomagmatic

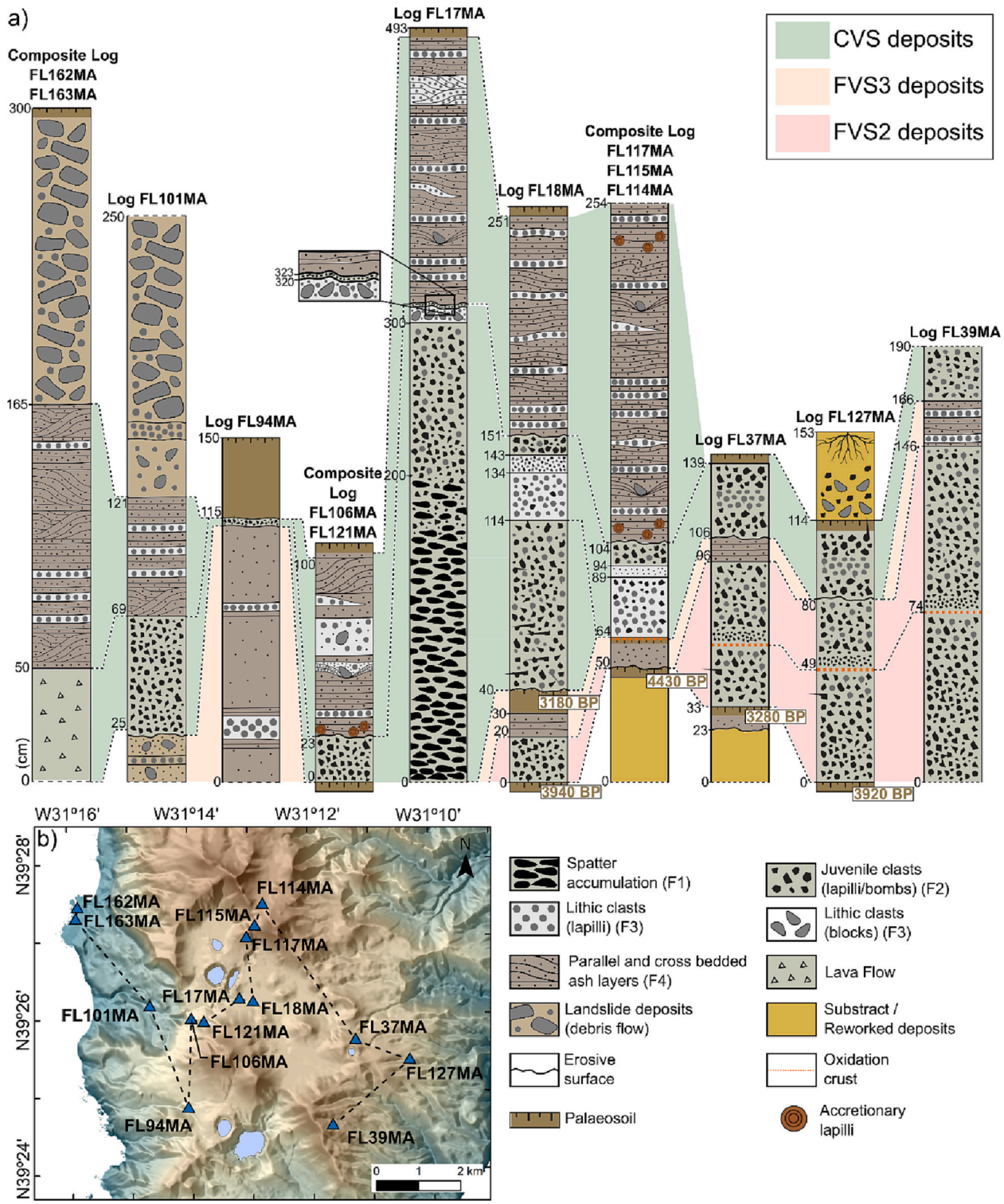

Fig. 7. a) Correlation panel of the representative CVS sequences. Dashed lines correlate the different products and the shaded areas identify the deposits of the different volcanic eruptions. White boxes indicate the radiocarbon ages obtained for the paleosols; b) location of the volcanic sequences used for correlations, plotted over the digital elevation model of the area. Dashed line shows the spatial correlation between the different sequences.

surge deposits (lithofacies F4, interpreted as part of CVS pyroclastic sequence) resting conformably over the A'a lava spines and clinker of the Fajã Grande delta is another evidence indicating that these products might be contemporary to the lavas emitted during the initial magmatic phase of CVS. The occurrence of volcanism between the two stages of gravitational collapse (see Fig. 5) is also attested by the presence of scoria lapilli/ash and phreatomagmatic fall deposits (F2 and F4 of Fig. 4g and Fig. 5e) unambiguously assigned to CVS (scoria from FL101MA outcrop plots in the same geochemical field of the other CVS tephras) between the deposits of the two different stages of collapse.

In summary, the effusive sequences of the magmatic phase of CVS eruption extended significantly (>4 km) westwards, cascaded over the initial landslide scar (landslide 1 in Fig. 1, Fig. 2 and Fig. 5) and infilled a valley carved into the landslide deposit, ultimately leading to the

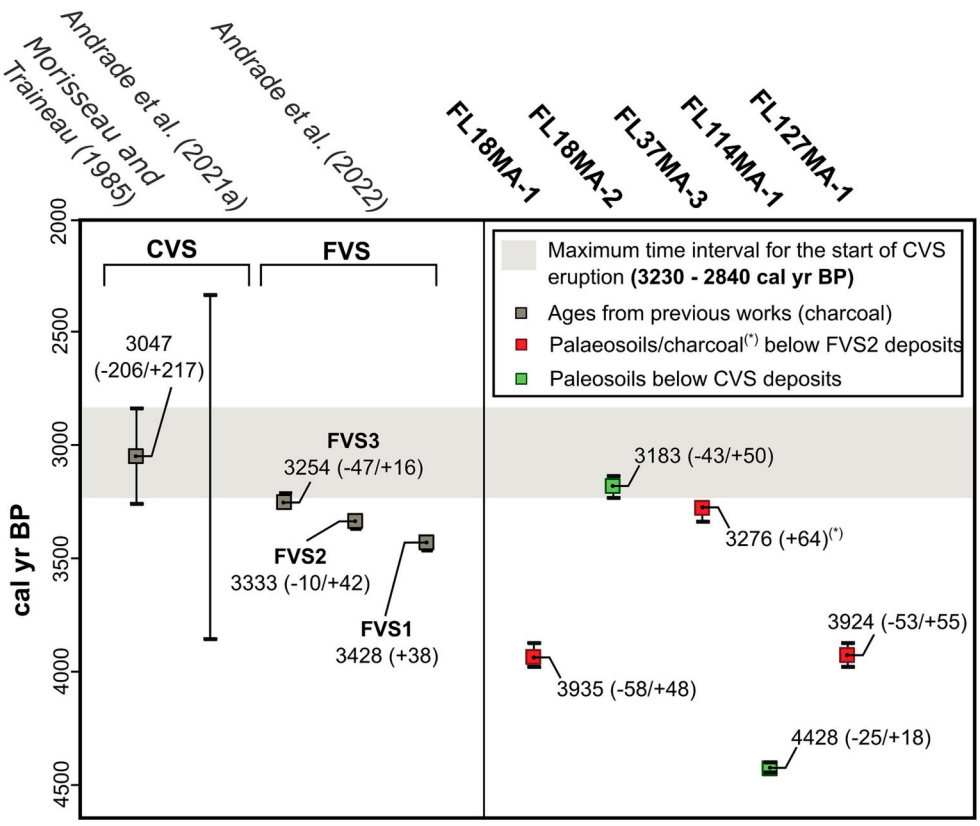

Fig. 8. Plot of the radiocarbon ages obtained from paleosols and charcoal below CVS pyroclastic sequence, and respective confidence range. On the left side the ages and respective confidence ranges attributed to CVS by Morisseau and Traineau (1985) and Andrade et al. (2021a), as well as the ages of the different FVS eruptions by Andrade et al. (2022) are plotted. The grey bar represents the temporal range for the onset of CVS eruption based on the ages obtained in this study and the previous works.

formation of the lava delta of Fajã Grande, which added ~0.5 km^2 to the island's coastline. The occurrence of landslide 2 (Figs. 1, 2 and 5) during the later stages or soon after the CVS eruption raises the possibility for a link between volcanic activity and the triggering of mass-wasting that needs to be further investigated.

The presence of accidental lithics in both lithofacies F1 and F2, and especially its increase towards the top of the deposits (e.g., FL17MA), suggests that during the initial magmatic phase of the eruption, explosions were expanding the volcanic conduits and/or crater walls were collapsing (Houghton and Smith, 1993; Sulpizio et al., 2005). This erosion and widening of the craters and conduits, likely associated with an increase in the eruption rate, shortly followed by a decrease that eventually allowed groundwater from the aquifer to enter the shallow plumbing system, resulted in the shift of eruptive style from Hawaiian-Strombolian to phreatomagmatic (Houghton and Schmincke, 1986, 1989; Gutmann, 2002; Gisbert et al., 2009). This change in the eruptive style was followed by successive phreatomagmatic explosions and vent migration, sometimes forming composite craters such as Lagoa Comprida (Fig. 9a), ultimately leading to the formation of the maars and tuff rings. Such transition of style from magmatic to phreatomagmatic is common in many mafic volcanoes (Gisbert et al., 2009; Di Traglia et al., 2009; Saucedo et al., 2017; Zanon and Viveiros, 2019; Geshi et al., 2019; Pedrazzi et al., 2022), including FVS at Flores Island (Andrade et al., 2022).

However, contrary to FVS, the stratigraphic sequence of CVS does not suggest an irreversible change in eruptive style. In most outcrops, the base of CVS sequence is characterized by an intercalation of scoriae and lithic fall deposits (Fig. 7), which suggests either a shift in the eruptive style over time or, that different vents were erupting at the same time but with different styles, with water playing a different role in each of them. This oscillation in eruptive styles, however, must have been short-lived, as the sequence ends with a thick phreatomagmatic deposit.

A detailed reconstruction of the sequence of events that took place during the explosive phase of CVS eruption is difficult to accomplish based on the limited exposure. However, since Lagoa Negra maar is intersected by the rim of Lagoa Comprida maar (Fig. 9b and c), it can be inferred that phreatomagmatism was initiated at Lagoa Negra. Accordingly, it is possible that for a brief period, phreatomagmatic explosions were occurring at Lagoa Negra while Lagoa Comprida was still producing magmatic explosions. Such simultaneous magmatic and phreatomagmatic processes are particularly common when magma-water interaction occurs at very shallow levels, where localised variations in vent geometry and/or hydrology can influence the magma/water ratio. Under these circumstances different conditions may prevail at adjacent vents, or two portions of a single vent, during one eruptive phase (Houghton and Schmincke, 1986). Quickly alternating discrete phreatomagmatic and Strombolian activity from a single vent or vent system has been recorded from several basaltic volcanoes (Houghton and Schmincke, 1986; van Otterloo et al., 2013; Saucedo et al., 2017). This might have also been the case of CVS, as attested by the alternation of scoria (F2) and lithic fall (F3) deposits observed in some outcrops, as well as by the shallow nature of the explosions (<200 m; Fig. 9d-h).

The gradual influx of groundwater into the shallow plumbing system caused the magma/water ratio to decrease and, at a certain threshold, phreatomagmatism became prevalent. Phreatomagmatic explosions continued, along a NE-SW-oriented fissure, forming Lagoa Comprida and Lagoa Seca maars and CVS south and east craters (tuff rings). The elongated shape of Lagoa Comprida (crater row) and its alignment with Lagoa Seca and CVS south crater (Fig. 9) suggest a dyke intrusion with eventual migration of the vents to the north, ultimately triggering the maar explosion of Lagoa Seca. A linear vent system was also described for FVS (Andrade et al., 2022), which suggests that fracture zones may have an important role in the propagation of magma at Flores Island and, more importantly, in the opening of vents during an eruption. This factor should be properly considered when constraining the source areas in volcanic hazard studies.

Based on geomorphological relationships, Lagoa Branca tuff ring is

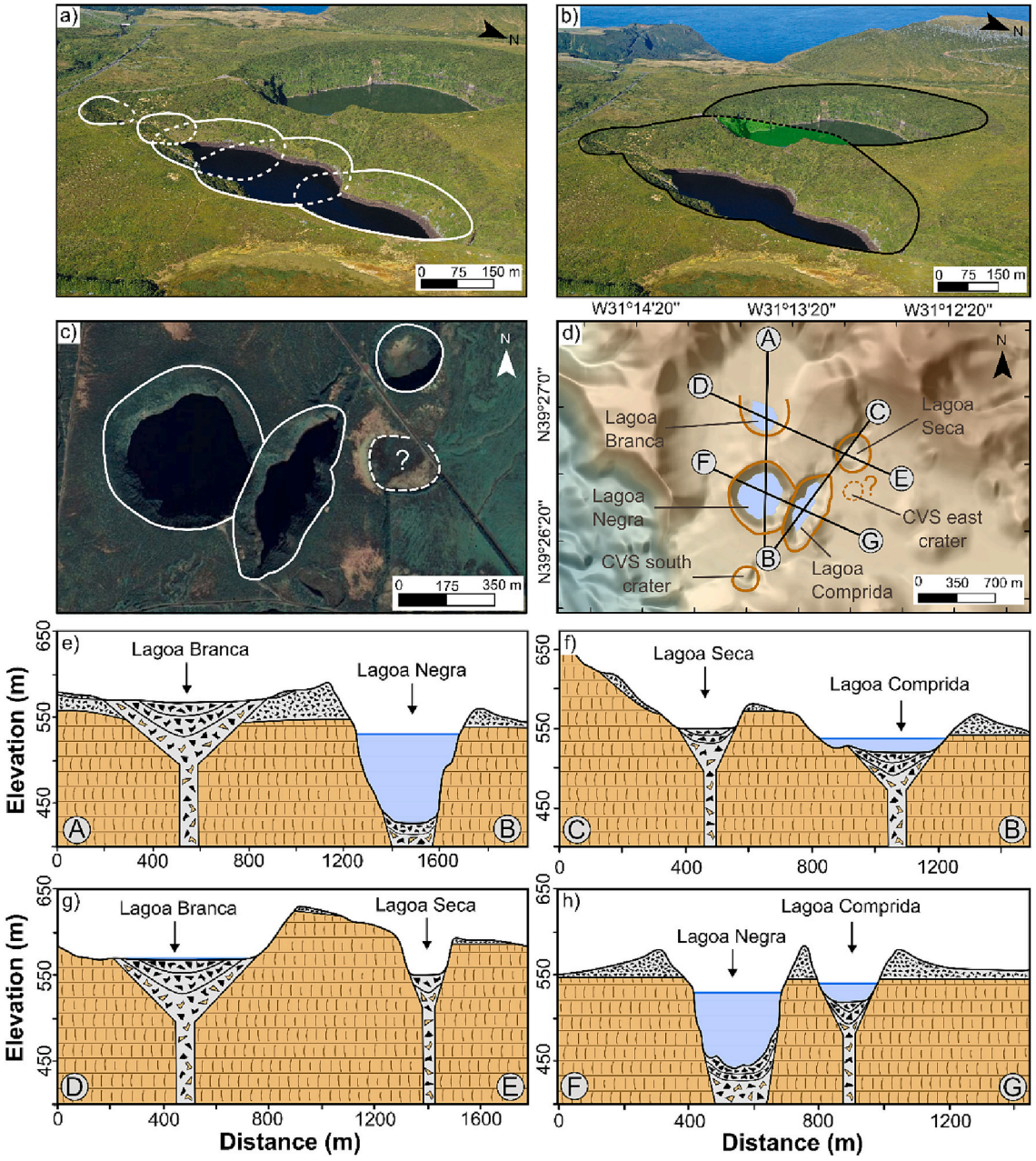

Fig. 9. Geometric relations between the craters of CVS; a) digital elevation model with a detailed view of CVS showing the different craters and the lines used to trace the profiles in panels e-h; b) photograph of Lagoa Comprida showing its composite morphology (crater row) resulting from discrete phreatomagmatic explosions along an eruptive fissure; c-d) photographs showing the geometric relations between Lagoa Negra and Lagoa Comprida maars, with Lagoa Negra being intersected by Lagoa Comprida; e-h) terrain profiles of CVS, showing geological interpretations of the relative ages of the different phreatomagmatic craters.

interpreted to record the last stage of the the CVS eruption. It is a very shallow crater (Fig. 9e and g) and, if formed at the early stages of the eruption, the large volume of material ejected during the formation of Lagoa Negra, Lagoa Comprida, and Lagoa Seca maars would have completely buried the low topography of Lagoa Branca tuff ring. Moreover, the formation of tuff rings is favoured by magma/water ratios close to 1:1 and maar-type explosions by ratios close to 3:1 (Lorenz, 1986) This reinforces the idea that Lagoa Branca may have formed during the final stage of the eruption, when the eruption rate was decreasing and the amount of water available in the system was higher than in early stages.

Based on the nature of the deposits, we infer that the final phase of the CVS eruption was characterized by discrete phreatomagmatic explosions, as attested by the well-bedded fabric of the upper deposits (F4), which show evidence for both vertical (fall deposits and ballistics) and lateral deposition (dilute PDC deposits). The thickness and internal structure of such deposits is spatially diverse, reflecting the complexity of the depositional processes and maybe the simultaneous activity of different vents.

All CVS craters were formed by relatively shallow explosions (<200 m), favouring the ejection of material from these craters (Valentine et al., 2014; Graettinger et al., 2015; Ort et al., 2018). Therefore, in the most proximal areas, volcanic sequences are expected to record interlayered deposits from multiple vents, especially considering the proximity of the different craters to each other. However, only the strongest and most efficient explosions would be capable to disperse fallout material to more distant areas. For this reason, we assume that in distal areas the lithic-rich fall layers of lithofacies F3 and F4 are mainly the

result of maar-forming explosions, especially those from Lagoa Negra and Lagoa Comprida. Weak eruptions, such as those forming Lagoa Branca, CVS south and east craters, ejected material that was essentially deposited as ballistics, mainly forming tuff rings around the craters.

The dilute PDC deposits present a great spatial variability in terms of thickness, grain size, and components. PDC deposits in the northern part of CVS (outcrops FL116MA and FL117MA; Fig. 4e-f) have abundant accretionary lapilli in the fine ash layers and juvenile particles are absent, suggesting that phreatomagmatic activity or even purely phreatic explosions were prevalent. Accordingly, and given the distribution of the PDC deposits to the north, we infer that they were likely deposited from dilute PDCs (surges) generated at Lagoa Branca, less likely Lagoa Seca.

In the south and western directions, PDCs were controlled by topography, cascading over the collapse scar of landslide 1 and eventually became channelled along the valley leading to Fajã Grande, following the same path as the lava flow produced during the initial magmatic phase of the eruption. The great thickness (>1 m; Fig. 4h) and grain size (clasts up to 10 cm) of the PDC deposits ~4 km away from the source area (e.g., outcrops FL162MA and FL163MA) suggest that the parent PDCs were capable of transporting coarse material along a considerable distance. Moreover, the high content of rounded scoriaceous particles and olivine crystals (accidental lithics) also shows that such PDCs were erosive and incorporated unconsolidated tephras mantling the topography, especially in proximal areas. Although linking PDC deposits to a specific source may be challenging, we interpret the PDC deposits of Fajã Grande as being sourced from explosions at Lagoa Negra, not only due to the proximity of Lagoa Negra maar to the cliff formed by landslide 1, but also due to the high content and large grain size of the scoriaceous particles, which can only be found in the vicinity of Lagoa Negra and Lagoa Comprida maars.

5.3. Reconstruction of eruption dispersal and physical parameters

In this section, we reconstruct the dispersal of the products of the CVS eruption and provide estimates of the main physical parameters. In proximal areas, different units of fall deposits (lithofacies F2 and F3) can be distinguished. However, further away from the source, the different fall deposits merge into a single undistinguishable deposit (e.g., outcrops FL158MA, FL127MA and FL37MA; Supplementary Fig. 2b-c and e). For that reason and taking into account that the lithic fall deposits sometimes also contain an important proportion of juveniles (scoria), we considered the different fall units as a whole to map tephra dispersal and determine physical parameters.

Isopach and isopleth maps show that CVS tephra fall deposits were dispersed along a single axis, southeast-oriented (Fig. 10a-c), suggesting that the wind was mainly blowing from northwest at the time of the eruption. This wind direction is consistent with the current wind pattern for the Azores region, which is dominated by westerly-blowing winds (Pimentel, 2006; Gaspar et al., 2015), but also with paleowind directions

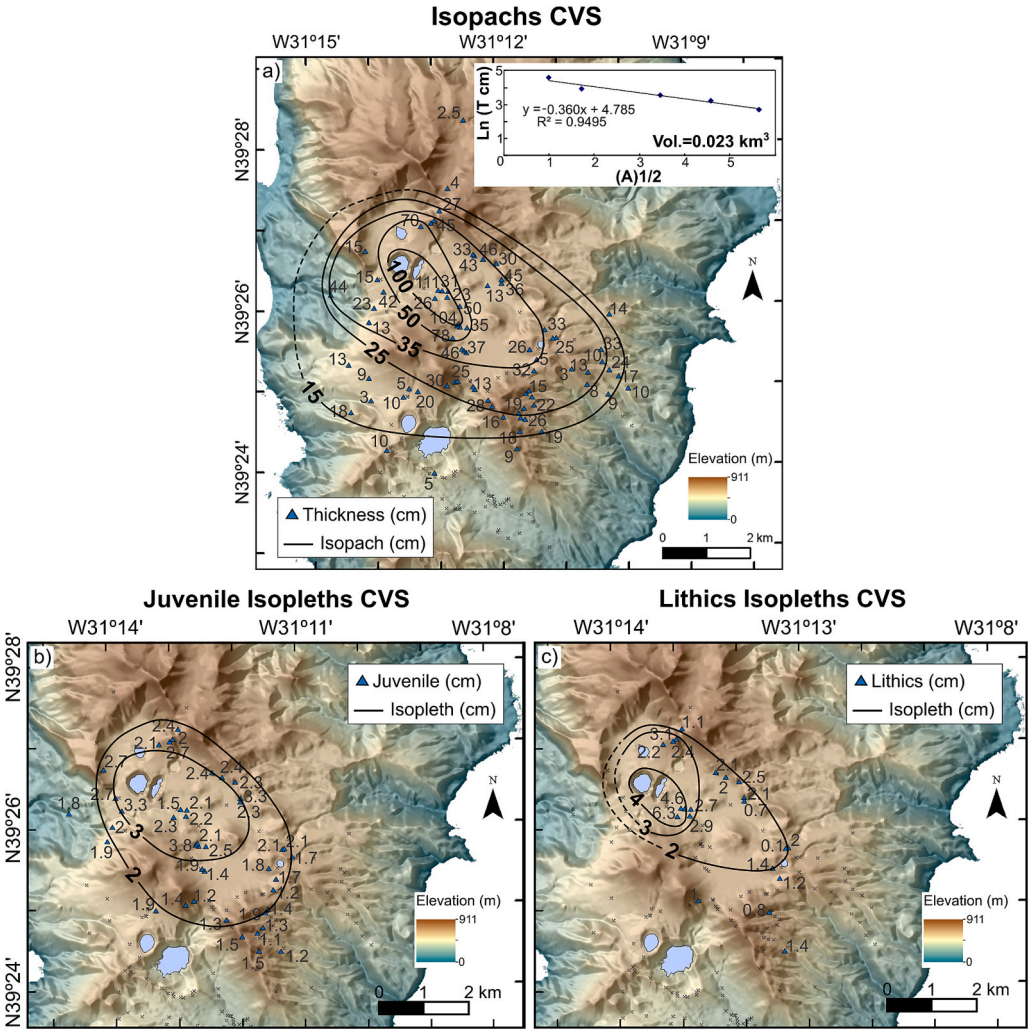

Fig. 10. a) Isopach map of CVS tephra fall deposit. Grey crosses represent field sites where the deposit is absent. The upper right diagram shows the log of thickness vs. square root of area for CVS tephra fall deposit; b) Isopleth map for juvenile clasts; and c) Isopleth map for lithic clasts.

reconstructed from tephra dispersal at Flores Island ~3000 years ago (FVS2 eruption; Andrade et al., 2022), Terceira Island ~2000 years ago (Self, 1976), and São Miguel Island, over the last 5000 years (Booth et al., 1978).

CVS isopach map shows a good exponential thinning of the deposit with distance from the source, as attested by the general regular spacing of the isopachs and by the good correlation of data points in the ln (thickness) vs. square root of the area (isopach area) diagram (Fig. 10a). Nevertheless, isopachs show some near-vent deviation (Fig. 10a) which may reflect the influence of ballistics in proximal areas. CVS tephras cover an area of 32 km^2 within the 15-cm-isopach, which yields a bulk volume of 0.023 km^3 (Table 2). Considering the small size of Flores Island (144 km^2 and only 12 km wide) and the proximity of the 15-cm-isopach to both east and west coastlines, we assume that an unknown portion of pyroclastic material was deposited offshore, as commonly reported for other explosive eruptions on small islands (e.g., Andronico and Pistolesi, 2010; Pimentel et al., 2015, 2021; Kueppers et al., 2019; Andrade et al., 2022). Accordingly, the estimated tephra bulk volume must be considered as minimum. Underestimations of tephra volumes are common in tropical and subtropical climates with strong winds and/or intense rainfall regimes, as the case of Flores, due to the high *syn*- and post-depositional reworking of subaerial exposures (Bolós et al., 2021).

The estimated tephra bulk volume indicates that CVS eruption corresponds to a volcanic explosivity index (VEI) 3 event (Newhall and Self, 1982). Based on the minimum and maximum values of measured tephra densities (see methods for details), the erupted mass was estimated between 1.635×10^{10} kg and 1.772×10^{10} kg, corresponding to a DRE volume of 0.006 km^3 (using a trachybasalt magma density of 2800 kg/m^3; Pimentel et al., 2016). CVS eruption is classified as an event with magnitude of 3.2 (Table 2).

Despite the apparent similarities between the magmatic phases of CVS and FVS2 eruptions, CVS involved a lower volume of magma (DRE volume FVS2 = 0.011 km^3 vs. DRE volume CVS = 0.006 km^3) with a slightly less evolved composition, which may have resulted in different eruptive dynamics. While FVS2 was a violent Strombolian eruption that developed a vertical eruption column (up to 9.4 km in height) that was strongly dispersed by the wind (Andrade et al., 2022), the small dispersion of CVS tephra fall deposits suggests that the eruption was characterized by pulsatory Hawaiian-style lava fountaining, and minor Strombolian-style explosions, without the development of a sustained vertical eruption column.

The CVS eruptive style transition from Hawaiian-Strombolian to phreatomagmatic is similar to that described for other small monogenetic volcanoes, e.g., Montsacopa volcano in the Catalan Volcanic Zone (Martí et al., 2011). Dilute PDCs produced during CVS phreatomagmatic activity had small runout extents, with the associated deposits being limited to the surrounding of CVS, except to the west, where PDCs descended upon the low topography of the Fajãzinha-Fajã Grande collapse, where they were channelled through the valley leading to Fajã Grande (Fig. 5). In all other directions PDC deposits are usually distributed radially, up to 1–2 km away from the CVS vents, but remained relatively confined within the floor of Sete Lagoas caldera.

Table 2
Summary of the physical parameters of CVS eruption.

Physical parameter	CVS eruption
Bulk volume (km^3)[1]	0.023
Volcanic explosivity index (VEI)[2]	3
Erupted mass ($x10^{10}$kg)[3]	1.635–1.772
Magnitude[4]	3.2
Dense rock equivalent (DRE) volume (km^3)[5]	0.006

[1] After Pyle (1989) modified by Fierstein and Nathenson (1992).
[2] After Newhall and Self (1982).
[3] Using minimum and maximum tephra bulk densities of 844 and 915 kg/m^3.
[4] After Pyle (2000).
[5] Using tephra bulk densities and trachybasalt magma density of 2800 kg/m^3.

Based on the volume of Lagoa Comprida, Lagoa Negra, and Lagoa Seca maars, we estimate a minimum value of 0.012 km^3 for the bedrock material ejected during the phreatomagmatic explosions.

5.4. Hazard implications

Recent works, including this study, show that Flores Island experienced at least six volcanic eruptions during the Holocene, therefore reinforcing the notion that Flores should be considered a potentially active volcanic island (Andrade et al., 2021a, 2022). Moreover, the geological record shows that these eruptions exhibited a variety of eruptive styles including Hawaiian-Strombolian, violent Strombolian and phreatomagmatic, sometimes with more than one style acting simultaneously as a result of differing magma-water interactions (Andrade et al., 2021a, 2022). Crucially, the stratigraphy of CVS also confirms that groundwater played an important role in the evolution of this volcanic system, by greatly influencing the explosivity of the eruption, namely by turning an initially mild Hawaiian-Strombolian eruption into a violent phreatomagmatic event capable of creating several maars, including the deepest maar of the Azores Archipelago – Lagoa Negra – which is 114 m deep (Andrade et al., 2021b).

Although a similar eruptive style transition has been reported for FVS (Andrade et al., 2022), the new findings on CVS eruption show that the influx of water into the shallow plumbing system can be determinant, particularly when small volumes of magma are involved and the vents are located into hydraulically-charged pre-existing volcanic sequences, as the one that fills Sete Lagoas caldera. In settings like this and owing to the several perched aquifers that permeate the volcanic edifice in this area, even small variations in eruption rate are enough to cause fluctuations around the threshold between Hawaiian-Strombolian and phreatomagmatic styles, leading to highly contrasting eruptive behaviours. This is particularly important since a sudden change in the eruptive style may result in a dramatic change of the volcanic hazard, unexpectedly threatening populations that were relatively safe from the threats posed by a largely effusive or mildly explosive basaltic eruption. This unpredictability is even greater when PDCs and/or lahars, two of the most hazardous volcanic phenomena that can be generated, take place.

A future magmatic eruption similar to the initial phase of CVS, sourced from the same general area, and characterized by Hawaiian lava fountaining and lava extrusion, would not pose a great threat to Flores' population, since tephra deposition would essentially be limited to the upland and uninhabited area of the island. Under this scenario, the only real threat would be to the Fajã Grande and Fajãzinha villages, which considering their proximity to CVS and the possibility of a lava flow, would probably need to be evacuated. Given their remote location (especially Fajãzinha that lacks a harbour) and considering that a lava flow could eventually block the access to the village, evacuating the area could become challenging, especially during the winter months when sea conditions are rough. However, a sudden shift in eruptive style from Hawaiian-Strombolian to phreatomagmatic could rapidly produce widespread PDCs, lahars, and directional blasts (Barberi et al., 1992), greatly increasing the threat to the local populations and making the management of the eruption crisis more challenging. The possibility of a combined threat of eruption and large-scale mass wasting should also not be underestimated, as the geological record of CVS suggests.

Finally, phreatomagmatism may have been recurrent at Flores, as evidenced by the recent eruptions of FVS and CVS but also by older phreatomagmatic craters, such as those of Lagoa da Lomba (>23,520 cal yr BP; Andrade et al., 2021a), Caldeirinha, and Caldeira Velha (undetermined Pleistocene ages; see Fig. 1 for location). Accordingly, and considering the abundance of superficial and groundwater existing at Flores, a good understanding of the subsurface geology of the island, including the distribution and hydraulic characteristics of the aquifers, is crucial to properly assess the volcanic hazards at Flores Island.

6. Conclusions

This study combined tephrostratigraphy, geomorphology, radiocarbon dating, and glass shard geochemistry to reconstruct the eruptive history of CVS, the youngest eruptive centre of Flores Island. The stratigraphy of CVS shows that its eruptive history was marked by a single eruption, taking place at ~3180 cal yr BP, after a period of volcanic quiescence of ~70 years (more information regarding Flores' previous eruptions can be found at Andrade et al., 2022). Such eruption was characterized by different eruptive styles, having shifted from Hawaiian-Strombolian to phreatomagmatic. The initial dominantly magmatic phase was characterized by lava fountaining and lava extrusion, having produced magmatic edifices in the sites where Lagoa Comprida and Lagoa Negra now stand. A large and final phreatomagmatic phase followed, being characterized by relatively shallow explosions, producing the different maars and tuff rings we see today.

A decrease in the eruption rate associated with the erosion and widening of the volcanic conduits seem to have been the main factors contributing for the entrance of water into the shallow plumbing system. Although magma-water interactions also happened in the past (Andrade et al., 2022), our new data show that water may play an important role during low explosivity/effusive eruptions taking place at hydraulically-charged volcanic terrains, and particularly when small volumes of magma are involved. Accordingly, in these settings, magma-water interactions may give rise to activity that is more explosive and less predictable, with clear hazard implications, which must be considered in future volcanic hazard assessments.

Supplementary data to this article can be found online at https://doi.org/10.1016/j.jvolgeores.2023.107806.

Funding

This work was funded by the Portuguese Fundação para a Ciência e a Tecnologia (FCT) I.P./MCTES through national funds (PIDDAC) – UIDB/50019/2020- IDL – and projects IF/01641/2015 MEGAWAVE, PTDC/CTA-GEO/0798/2020 HAZARDOUS. Preliminary fieldwork was also supported by project TH1530/6–1 funded by DFG - The German Research Foundation. MA is funded by FCT through her doctoral grant (SFRH/BD/138261/2018). AH is funded by the Spanish Ministry of Science and Innovation through the Ramón y Cajal Scheme [RYC2020–029253-I].

Credit author statement

Mariana Andrade: Conceptualization, Data curation, Formal analysis, Investigation, Methodology, Writing - original draft, Writing - review & editing. **Ricardo Ramalho**: Conceptualization, Data curation, Investigation, Methodology, Writing - review & editing. **Adriano Pimentel**: Conceptualization, Data curation, Investigation, Methodology, Writing - review & editing. **Steffen Kutterolf**: Data curation, Formal analysis, Methodology, Writing - review & editing. **Armand Hernández**: Conceptualization, Data curation, Investigation, Methodology, Writing - review & editing.

Declaration of Competing Interest

The authors declare that they have no known competing financial interests or personal relationships that could have appeared to influence the work reported in this paper.

Data availability

Data will be made available on request.

Acknowledgements

We acknowledge the GEOMAR Helmholtz Centre for providing the facilities and technical support during the geochemical analysis. We thank M. Antunes at Secretaria Regional do Turismo e Transportes for providing the digital altimetric database used in this study. We also acknowledge Serviços Florestais das Flores e Corvo, as well as Câmara Municipal das Lajes das Flores, for their support in field logistics and access to some of the outcrops. We thank Bruno Ázera for providing the aerial photograph of CVS.

References

Andrade, C., Cruz, J., Viveiros, F., Coutinho, R., 2019. CO2 Flux from Volcanic Lakes in the Western Group of the Azores Archipelago (Portugal). Water 11, 599. https://doi.org/10.3390/w11030599.

Andrade, M., Ramalho, R.S., Pimentel, A., Hernández, A., Kutterolf, S., Sáez, A., Benavente, M., Raposeiro, P.M., Giralt, S., 2021a. Unraveling the Holocene Eruptive history of Flores Island (Azores) through the Analysis of Lacustrine Sedimentary Records. Front. Earth Sci. 9, 738178 https://doi.org/10.3389/feart.2021.738178.

Andrade, C., Viveiros, F., Cruz, J.V., Coutinho, R., 2021b. Global carbon dioxide output of volcanic lakes in the Azores archipelago, Portugal. J. Geochem. Explor. 229, 106835 https://doi.org/10.1016/j.gexplo.2021.106835.

Andrade, M., Pimentel, A., Ramalho, R., Kutterolf, S., Hernández, A., 2022. The recent volcanism of Flores Island (Azores): Stratigraphy and eruptive history of Funda Volcanic System. J. Volcanol. Geotherm. Res. 432, 107706 https://doi.org/10.1016/j.jvolgeores.2022.107706.

Andronico, D., Lodato, L., 2005. Effusive activity at Mount Etna Volcano (Italy) during the 20th Century: a Contribution to Volcanic Hazard Assessment. Nat. Hazards 36, 407–443. https://doi.org/10.1007/s11069-005-1938-2.

Andronico, D., Pistolesi, M., 2010. The November 2009 paroxysmal explosions at Stromboli. J. Volcanol. Geotherm. Res. 196, 120–125. https://doi.org/10.1016/j.jvolgeores.2010.06.005.

Azevedo, J.M.M., 1998. Geologia e Hidrogeologia da Ilha das Flores (Doctoral Thesis). Universidade de Coimbra, Coimbra.

Azevedo, J.M.M., Portugal Ferreira, M.R., 1999. Volcanic gaps and subaerial records ofpalaeo-sea-levels on Flores Island (Azores): tectonic andmorphological implications. J. Geodyn. 28, 117–129. https://doi.org/10.1016/S0264-3707(98)00032-5.

Azevedo, J.M.M., Portugal Ferreira, M.R., 2006. The volcanotectonic evolution of Flores Island, Azores (Portugal). J. Volcanol. Geotherm. Res. 156, 90–102. https://doi.org/10.1016/j.jvolgeores.2006.03.011.

Azevedo, J.M.M., Portugal Ferreira, M.R., Ávila Martins, J., 1991. The Emergent Volcanism of Flores Island, Azores (Portugal). Arquipélago. Bolet. Universidade dos Açores: Ciências da Natureza 9, 37–46.

Ball, J.L., 2022. Stratigraphy and eruption history of maars in the Clear Lake Volcanic Field, California. Front. Earth Sci. 10, 911129 https://doi.org/10.3389/feart.2022.911129.

Barberi, F., Bertagnini, A., Landi, P., Principe, C., 1992. A review on phreatic eruptions and their precursors. J. Volcanol. Geotherm. Res. 52, 231–246. https://doi.org/10.1016/0377-0273(92)90046-G.

Barsotti, S., Parks, M.M., Pfeffer, M.A., Óladóttir, B.A., Barnie, T., Titos, M.M., Jónsdóttir, K., Pedersen, G.B.M., Hjartardóttir, Á.R., Stefansdóttir, G., Johannsson, T., Arason, Þ., Gudmundsson, M.T., Oddsson, B., Þrastarson, R.H., Ófeigsson, B.G., Vogfjörd, K., Geirsson, H., Hjörvar, T., von Löwis, S., Petersen, G.N., Sigurðsson, E.M., 2023. The eruption in Fagradalsfjall (2021, Iceland): how the operational monitoring and the volcanic hazard assessment contributed to its safe access. Nat. Hazards. https://doi.org/10.1007/s11069-022-05798-7.

Bolós, X., Macias, J.L., Ocampo-Díaz, Y.Z.E., Tinoco, C., 2021. Implications of reworking processes on tephra distribution during volcanic eruptions: the case of Parícutin (1943–1952, western Mexico). Earth Surf. Process. Landf. 46, 3143–3157. https://doi.org/10.1002/esp.5222.

Booth, B., Croasdale, R., Walker, G.P.L., 1978. A quantitative study of five thousand years of volcanism on Sao Miguel, Azores. Phil. Trans. R. Soc. Lond. A 288, 271–319. https://doi.org/10.1098/rsta.1978.0018.

Chester, D., Duncan, A., Coutinho, R., Wallenstein, N., Branca, S., 2017. Communicating Information on Eruptions and their Impacts from the Earliest Times until the late Twentieth Century. In: Fearnley, C.J., Bird, D.K., Haynes, K., McGuire, W.J., Jolly, G. (Eds.), Observing the Volcano World, Advances in Volcanology. Springer International Publishing, Cham, pp. 419–443. https://doi.org/10.1007/11157_2016_30.

Di Traglia, F., Cimarelli, C., de Rita, D., Gimeno Torrente, D., 2009. Changing eruptive styles in basaltic explosive volcanism: examples from Croscat complex scoria cone, Garrotxa Volcanic Field (NE Iberian Peninsula). J. Volcanol. Geotherm. Res. 180, 89–109. https://doi.org/10.1016/j.jvolgeores.2008.10.020.

EMODnet Bathymetry Consortium, 2018. EMODnet Digital Bathymetry (DTM 2018) [WWW Document]. URL. https://doi.org/10.12770/18ff0d48-b203-4a65-94a9-5fd8b0ec35f6.

Fierstein, J., Nathenson, M., 1992. Another look at the calculation of fallout tephra volumes. Bull. Volcanol. 54, 156–167. https://doi.org/10.1007/BF00278005.

Gaspar, J.L., Queiroz, G., Ferreira, T., Medeiros, A.R., Goulart, C., Medeiros, J., 2015. Chapter 4 Earthquakes and volcanic eruptions in the Azores region: geodynamic

implications from major historical events and instrumental seismicity. Memoirs 44, 33–49. https://doi.org/10.1144/M44.4.
Genske, F.S., Beier, C., Stracke, A., Turner, S.P., Pearson, N.J., Hauff, F., Schaefer, B.F., Haase, K.M., 2016. Comparing the nature of the western and eastern Azores mantle. Geochim. Cosmochim. Acta 172, 76–92. https://doi.org/10.1016/j.gca.2015.08.019.
Geshi, N., Németh, K., Noguchi, R., Oikawa, T., 2019. Shift from magmatic to phreatomagmatic explosions controlled by the lateral evolution of a feeder dike in the Suoana-Kazahaya eruption, Miyakejima Volcano, Japan. Earth Planet. Sci. Lett. 511, 177–189. https://doi.org/10.1016/j.epsl.2019.01.038.
Gisbert, G., Gimeno, D., Fernandez-Turiel, J.L., 2009. Eruptive mechanisms of the Puig De La Garrinada volcano (Olot, Garrotxa volcanic field, Northeastern Spain): a methodological study based on proximal pyroclastic deposits. J. Volcanol. Geotherm. Res. 180, 259–276. https://doi.org/10.1016/j.jvolgeores.2008.12.018.
Graettinger, A.H., Valentine, G.A., Sonder, I., Ross, P.-S., White, J.D.L., 2015. Facies distribution of ejecta in analog tephra rings from experiments with single and multiple subsurface explosions. Bull. Volcanol. 77, 66. https://doi.org/10.1007/s00445-015-0951-x.
Gutmann, J.T., 2002. Strombolian and effusive activity as precursors to phreatomagmatism: eruptive sequence at maars of the Pinacate volcanic field, Sonora, Mexico. J. Volcanol. Geotherm. Res. 113, 345–356. https://doi.org/10.1016/S0377-0273(01)00265-7.
Hildenbrand, A., Marques, F.O., Catalão, J., 2018. Large-scale mass wasting on small volcanic islands revealed by the study of Flores Island (Azores). Sci. Rep. 8, 13898. https://doi.org/10.1038/s41598-018-32253-0.
Houghton, B.F., Schmincke, H.-U., 1986. Mixed deposits of simultaneous strombolian and phreatomagmatic volcanism: Rothenberg volcano, east Eifel volcanic field. J. Volcanol. Geotherm. Res. 30, 117–130. https://doi.org/10.1016/0377-0273(86)90069-7.
Houghton, B.F., Schmincke, H.-U., 1989. Rothenberg scoria cone, East Eifel: a complex Strombolian and phreatomagmatic volcano. Bull. Volcanol. 52, 28–48. https://doi.org/10.1007/BF00641385.
Houghton, B.F., Smith, R.T., 1993. Recycling of magmatic clasts during explosive eruptions: estimating the true juvenile content of phreatomagmatic volcanic deposits. Bull. Volcanol. 55, 414–420. https://doi.org/10.1007/BF00302001.
Hunt, J.B., Hill, P.G., 2001. Tephrological implications of beam size?Sample-size effects in electron microprobe analysis of glass shards. J. Quat. Sci. 16, 105–117. https://doi.org/10.1002/jqs.571.
Jarosewich, E., Nelen, J.A., Norberg, J.A., 1980. Reference Samples for Electron Microprobe Analysis*. Geostand. Geoanal. Res. 4, 43–47. https://doi.org/10.1111/j.1751-908X.1980.tb00273.x.
Kisaka, M., Fontijn, K., Shemsanga, C., Tomašek, I., Gaduputi, S., Debaille, V., Delcamp, A., Kervyn, M., 2021. The late Quaternary eruptive history of Meru volcano, northern Tanzania. J. Volcanol. Geotherm. Res. 417, 107314 https://doi.org/10.1016/j.jvolgeores.2021.107314.
Kueppers, U., Pimentel, A., Ellis, B., Forni, F., Neukampf, J., Pacheco, J., Perugini, D., Queiroz, G., 2019. Biased volcanic hazard assessment due to incomplete eruption records on Ocean Islands: an example of Sete Cidades Volcano. Azores. Front. Earth Sci. 7, 122. https://doi.org/10.3389/feart.2019.00122.
Kutterolf, S., Freundt, A., Burkert, C., 2011. Eruptive history and magmatic evolution of the 1.9 kyr Plinian dacitic Chiltepe Tephra from Apoyeque volcano in west-Central Nicaragua. Bull. Volcanol. 73, 811–831. https://doi.org/10.1007/s00445-011-0457-0.
LeBas, M.J., Maitre, R.W.L., Streckeisen, A., Zanettin, B., IUGS Subcommission on the Systematics of Igneous Rocks, 1986. A Chemical Classification of Volcanic Rocks based on the Total Alkali-Silica Diagram. J. Petrol. 27, 745–750. https://doi.org/10.1093/petrology/27.3.745.
Lorenz, V., 1986. On the growth of maars and diatremes and its relevance to the formation of tuff rings. Bull. Volcanol. 48, 265–274. https://doi.org/10.1007/BF01081755.
Martí, J., Planagumà, L., Geyer, A., Canal, E., Pedrazzi, D., 2011. Complex interaction between Strombolian and phreatomagmatic eruptions in the Quaternary monogenetic volcanism of the Catalan Volcanic Zone (NE of Spain). J. Volcanol. Geotherm. Res. 201, 178–193. https://doi.org/10.1016/j.jvolgeores.2010.12.009.
Martí, J., Becerril, L., Rodríguez, A., 2022. How long-term hazard assessment may help to anticipate volcanic eruptions: the case of La Palma eruption 2021 (Canary Islands). J. Volcanol. Geotherm. Res. 431, 107669 https://doi.org/10.1016/j.jvolgeores.2022.107669.
McLean, D., Albert, P.G., Suzuki, T., Nakagawa, T., Kimura, J.-I., Chang, Q., MacLeod, A., Blockley, S., Staff, R.A, Yamada, K., Kitaba, I., Haraguchi, T., Kitagawa, J., Smith, V. C., 2020. Refining the eruptive history of Ulleungdo and Changbaishan volcanoes (East Asia) over the last 86 kyrs using distal sedimentary records. J. Volcanol. Geotherm. Res. 389, 106669 https://doi.org/10.1016/j.jvolgeores.2019.106669.
Métrich, N., Zanon, V., Créon, L., Hildenbrand, A., Moreira, M., Marques, F.O., 2014. Is the 'Azores Hotspot' a Wetspot? Insights from the Geochemistry of Fluid and Melt Inclusions in Olivine of Pico Basalts. J. Petrol. 55, 377–393. https://doi.org/10.1093/petrology/egt071.
Morisseau, M., Traineau, H., 1985. Mise en évidence d'une activité hydromagmatique holocène sur l'île de Flores (Açores). Comptes rendus de l'Académie des sciences. In: Série 2, Mécanique, Physique, Chimie, Sciences de l'univers, Sciences de la Terre, 301, pp. 1309–1314.
Newhall, C.G., Self, S., 1982. The volcanic explosivity index (VEI) an estimate of explosive magnitude for historical volcanism. J. Geophys. Res. 87, 1231. https://doi.org/10.1029/JC087iC02p01231.
Ort, M.H., Lefebvre, N.S., Neal, C.A., McConnell, V.S., Wohletz, K.H., 2018. Linking the Ukinrek 1977 maar-eruption observations to the tephra deposits: New insights into maar depositional processes. J. Volcanol. Geotherm. Res. 360, 36–60. https://doi.org/10.1016/j.jvolgeores.2018.07.005.
Pedrazzi, D., Cerda, D., Geyer, A., Martí, J., Aulinas, M., Planagumà, L., 2022. Stratigraphy and eruptive history of the complex Puig de La Banya del Boc monogenetic volcano, Garrotxa Volcanic Field. J. Volcanol. Geotherm. Res. 423, 107460 https://doi.org/10.1016/j.jvolgeores.2021.107460.
Pimentel, A., 2006. Influence of wind patterns on the dispersal of volcanic plumes in the Azores region: Test study of the 1630 eruption of Furnas Volcano (S. Miguel, Azores). In: 04983. Presented at the European Geosciences Union. Geophysical Research Abstracts, Vienna.
Pimentel, A., Pacheco, J., Self, S., 2015. The ~1000-years BP explosive eruption of Caldeira Volcano (Faial, Azores): the first stage of incremental caldera formation. Bull. Volcanol. 77, 42. https://doi.org/10.1007/s00445-015-0930-2.
Pimentel, A., Zanon, V., de Groot, L.V., Hipólito, A., Di Chiara, A., Self, S., 2016. Stress-induced comenditic trachyte effusion triggered by trachybasalt intrusion: multidisciplinary study of the AD 1761 eruption at Terceira Island (Azores). Bull. Volcanol. 78, 22. https://doi.org/10.1007/s00445-016-1015-6.
Pimentel, A., Self, S., Pacheco, J.M., Jeffery, A.J., Gertisser, R., 2021. Eruption style, Emplacement Dynamics and Geometry of Peralkaline Ignimbrites: Insights from the Lajes-Angra Ignimbrite Formation, Terceira Island. Azores. Front. Earth Sci. 9, 673686 https://doi.org/10.3389/feart.2021.673686.
Pyle, D.M., 1989. The thickness, volume and grainsize of tephra fall deposits. Bull. Volcanol. 51, 1–15. https://doi.org/10.1007/BF01086757.
Pyle, D.M., 2000. Sizes of volcanic eruptions. In: Encyclopedia of Volcanoes. Academic Press, San Diego, pp. 263–269.
Ramalho, R.S., Quartau, R., Trenhaile, A.S., Mitchell, N.C., Woodroffe, C.D., Ávila, S.P., 2013. Coastal evolution on volcanic oceanic islands: a complex interplay between volcanism, erosion, sedimentation, sea-level change and biogenic production. Earth Sci. Rev. 127, 140–170. https://doi.org/10.1016/j.earscirev.2013.10.007.
Saucedo, R., Macías, J.L., Ocampo-Díaz, Y.Z.E., Gómez-Villa, W., Rivera-Olguín, E., Castro-Govea, R., Sánchez-Núñez, J.M., Layer, P.W., Torres Hernández, J.R., Carrasco-Núñez, G., 2017. Mixed magmatic–phreatomagmatic explosions during the formation of the Joya Honda maar, San Luis Potosí, Mexico. SP 446, 255–279. https://doi.org/10.1144/SP446.11.
Scarpa, R., Gasparini, P., 1996. A Review of Volcano Geophysics and Volcano-monitoring Methods. In: Monitoring and Mitigation of Volcano Hazards. Springer, Berlin Heidelberg, Berlin, Heidelberg, pp. 3–22. https://doi.org/10.1007/978-3-642-80087-0_1.
Secretaria Regional do Ambiente e do Mar, 2012. Plano de Gestão da Região Hidrográfica dos Açores RH9 - Caracterização da situação de referência e diagnóstico, vol. 8. Açores.
Self, S., 1976. The recent volcanology of Terceira, Azores. JGS 132, 645–666. https://doi.org/10.1144/gsjgs.132.6.0645.
Stuiver, M., Reimer, P.J., Reimer, R., 1993. CALIB rev. 8. Radiocarbon, 35, 215-230. [WWW program]. at. http://_calib.org. Accessed January 2021.
Sulpizio, R., Mele, D., Dellino, P., Volpe, L.L., 2005. A complex, Subplinian-type eruption from low-viscosity, phonolitic to tephri-phonolitic magma: the AD 472 (Pollena) eruption of Somma-Vesuvius, Italy. Bull. Volcanol. 67, 743–767. https://doi.org/10.1007/s00445-005-0414-x.
Taddeucci, J., Edmonds, M., Houghton, B., James, M.R., Vergniolle, S., 2015. Hawaiian and strombolian eruptions. In: The Encyclopedia of Volcanoes. Elsevier, pp. 485–503. https://doi.org/10.1016/B978-0-12-385938-9.00027-4.
Valentine, G.A., Graettinger, A.H., Sonder, I., 2014. Explosion depths for phreatomagmatic eruptions. Geophys. Res. Lett. 41, 3045–3051. https://doi.org/10.1002/2014GL060096.
van Otterloo, J., Cas, R.A.F., Sheard, M.J., 2013. Eruption processes and deposit characteristics at the monogenetic Mt. Gambier Volcanic complex, SE Australia: implications for alternating magmatic and phreatomagmatic activity. Bull. Volcanol. 75, 737. https://doi.org/10.1007/s00445-013-0737-y.
Zanon, V., Viveiros, F., 2019. A multi-methodological re-evaluation of the volcanic events during the 1580 CE and 1808 eruptions at São Jorge Island (Azores Archipelago, Portugal). J. Volcanol. Geotherm. Res. 373, 51–67. https://doi.org/10.1016/j.jvolgeores.2019.01.028.